DEVELOPMENT OF FLEXIBLE SENSORS WITH CONJUGATED POLYMERS

by

Aybüke Büşra Özer

Submitted to the Graduate School of Engineering and Natural Sciences

in partial fulfillment of

the requirements for the degree of Master of Science

Sabanci University

Spring 2023

DEVELOPMENT OF FLEXIBLE SENSORS WITH CONJUGATED POLYMERS

APPROVED BY:

DATE OF APPROVAL:

ABSTRACT

DEVELOPMENT OF FLEXIBLE SENSORS WITH CONJUGATED POLYMERS

Aybüke Büşra Özer

Master of Science Dissertation, July 2023

Supervisor: Asst. Prof. Eric TAN

Keywords: Flexible sensors, conjugated polymers, interdigitated electrodes (IDE), electrochemical sensors

Flexible electrode-based sensors are a specific type of sensing technology that incorporates flexible and bendable materials as the sensing elements. Unlike conventional rigid electrodes, these sensors are designed to adapt to irregular surfaces or be integrated into flexible substrates, enabling their utilization in various applications where flexibility and conformability are essential.

This thesis study aims to develop flexible sensors by integrating conjugated polymers with conductive surfaces. To pursue this objective, two distinct sensor systems were developed and investigated for their potential applications. Initially, an electrochemical pH sensor with a Polyaniline (PANI) coating was designed. The pH sensitivity of the sensor was evaluated by performing open-circuit potential measurements using a potentiostat. The second system involved an interdigitated electrode (IDE) based gas sensor coated with Polydiacetylene (PDA). The sensitivity of the gas sensor was assessed by monitoring the changes in impedance values using an LCR meter. Both sensor systems were fabricated by depositing patterned silver (Ag) electrodes onto PET film using the E-beam evaporation method, then applying the respective responsive sensing materials using the drop cast method. The results demonstrated the successful realization of a

flexible PANI-coated pH sensor capable of detecting various pH values and a PDA-coated gas sensor exhibiting sensitivity towards acetic acid. These findings contribute to the advancement of flexible sensor technologies for health and food-related potential applications.

ÖZET

KONJUGE POLİMERLERLE ESNEK SENSÖRLERİN GELİŞTİRİLMESİ

Aybüke Büşra ÖZER

Yüksek Lisans Tezi, Temmuz 2023

Tez Danışmanı: Dr. Öğr. Üyesi Eric TAN

Anahtar Kelimeler: Esnek sensörler, konjuge polimerler, aralıklı elektrotlar (IDE), elektrokimyasal sensörler

Esnek elektrot tabanlı sensörler, esnek ve bükülebilir malzemeleri içeren özel bir algılama teknolojisidir. Geleneksel sert elektrotlardan farklı olarak, bu sensörler düzensiz yüzeylere uyum sağlamak veya esnek alt tabakalara entegre edilmek üzere tasarlanmıştır, bu da esneklik ve uyum sağlama gerektiren çeşitli uygulamalarda kullanılmalarını sağlar.

Bu tez çalışması, konjuge polimerlerin iletken yüzeylerle entegrasyonuyla esnek sensörlerin geliştirilmesini amaçlamaktadır. Bu hedef doğrultusunda, açık devre potansiyeli ölçümleri yaparak farklı pH değerlerini değerlendirilen Polianilin (PANI) kaplamalı bir elektrokimyasal pH sensörü tasarlandı. İkinci sistem ise Polidiasetilen (PDA) ile kaplanmış aralıklı elektrot (IDE) tabanlı bir gaz sensörünü içermekteydi. Gaz sensörünün duyarlılığı, LCR metre kullanarak empedans değerlerindeki değişikliklerin izlenmesiyle değerlendirildi.

Her iki sensör sistemi, E-ışını buharlaştırma yöntemi kullanılarak PET film üzerine gümüş (Ag) elektrotların oluşturulması ve ardından ilgili duyarlı algılama malzemelerinin damlatma yöntemiyle uygulanmasıyla üretildi. Sonuçlar, çeşitli pH değerlerini algılayabilen esnek PANI kaplamalı bir pH sensörünün başarılı bir şekilde gerçekleştirildiğini ve asetik asit karşısında duyarlılık gösteren PDA kaplamalı bir gaz sensörünün olduğunu göstermiştir. Bu bulgular, sağlık ve gıda gibi alanlar potansiyel uygulamalarda esnek sensör teknolojilerinin ilerlemesine katkıda bulunmaktadır.

ACKNOWLEDGEMENTS

I would like to emphasize my sincere appreciation to everyone who supported me during this MSc thesis process. I would also like to thank the faculty members of Sabancı University, with special mention to my advisors, Eric Tan and Hande Cıngıl Tan. Their wealth of knowledge, mentorship, and academic insights have significantly enhanced my comprehension of the subject matter. Furthermore, I am thankful to my teammates Tayyaba Shaikh, Gizem Beliktay, Rana Golshei and Ceren Mitmit, who willingly dedicated their time and efforts to participate in my thesis work. I am grateful to my family members Tuba Aysenem Özer, İrfan Özer, Ayşe Özer and Fatih Turgut Özer, my friends Gülşah Yıldız, Büşra Elif Kıvrak, Cemile Uslu, Gülnur Şener and Sümeyye Narin for their unwavering support, encouragement and understanding throughout this challenging endeavour. I feel fortunate to have had the opportunity to complete this MSc thesis with your support successfully.

Finally, I thank the Tubitak 1004 Project NANOSIS for the scholarship and research funding.

TABLE OF CONTENT

LIST OF FIGURES

LIST OF ABBREVIATIONS

PDAs	:	Polydiacetylenes
PANI	:	Polyaniline
PET	:	Polyethylene terephthalate
Z	:	Impedance
PVD	:	Physical Vapor Deposition
ES	:	Emeraldine Salt
APS	:	Ammonium Persulfate
TRIS	:	Tris(hydroxymethyl)aminomethane
SDBS	:	Sodium Dodecylbenzene Sulphonate
THF	:	Tetrahydrofuran
IDE	:	Interdigitated Electrode
PEO	:	Polyethylene Oxide
SEM	:	Scanning Electron Microscopy
VOC	:	Volatile Organic Compound
ES	:	Emeraldine Salt
sccm	:	standard cubic centimeters per minute

CHAPTER 1. INTRODUCTION

1.1. Flexible Sensors

Flexible sensors typically comprise a pliable substrate, a conductive electrode, a sensing element, and sometimes an enclosure material. Both the electrode and sensing materials must exhibit stable performance to ensure reliable electrical functionality in flexible sensors even under significant and repetitive deformation [1]. Using flexible/stretchable electronics in device engineering has enabled the development of thin, light, stretchable, and foldable sensors. These sensors are widely employed in diverse fields, from robotics to healthcare monitoring.

1.1.1 Substrates

The substrate material is one of the significant elements in producing flexible devices. Polymers, ultrathin glass [2], and metal foil [3] are often employed as substrates because of their high mechanical flexibility, thermal stability, and superior chemical resistance[4, 5]. Plastic substrates have good flexibility and hardness comparable to metal foils and optical transmittance comparable to thin glass. Polyethylene terephthalate (PET), polyethylene naphthalate (PEN) [6], and polyimide (PI) [7] are commonly preferred as flexible polymer substrates.

PET is an excellent commercial thermoplastic polymer resin of the polyester family. PET substrate has garnered interest in various applications, including packaging [8], display technology [9], and as a substrate for flexible electronics because of its low cost, high transparency, great moisture resistance, outstanding spin ability, surface inertness, excellent mechanical properties and good thermal stability [10]. The PET film is a reliable substrate for depositing functional layers, enabling the integration of different materials and components necessary for creating an active surface to develop flexible sensors.[11] The choice of PET film as a substrate offers advantages such as ease of processing, compatibility with deposition techniques, and overall performance in terms of mechanical integrity and barrier properties.

1.1.2 Conductive Surface (Electrode)

Electrochemical sensors detect chemical changes on the active surface by converting the chemical changes to electrical signals. In this system, the electrodes measure electrical detection signals and an interface for applying an electric field to the samples. These electrical signals might be impedance (Z), resistance (R), capacitance (C), or electrical spectroscopy.[12-14]

Planar electrodes are commonly used for miniaturization of conductimetric sensor design. The advantage of planar electrodes is that they are designed in desired shape and size using CAD programs such as SolidWorks. These low-cost systems can also use various applications without requiring substantial modifications to the sensor design.[15]

The fastest-growing category of chemical sensors is electrochemical sensors. Chemical sensors can be defined as compact devices that utilize a chemical interaction or process between the analyte and the sensor device to convert chemical or biochemical information, whether quantitative or qualitative, into a signal that possesses analytical utility.[16, 17] Chemical sensors consist of a physical transducer and a chemically sensitive layer. These sensors operate by detecting changes in the characteristics of the chemical layer, which are then measured by the instrument through the emission of energy signals such as thermal, electrical, or optical signals.[18] Several deposition techniques, such as screen printing, inkjet printing, and electrodeposition, have been developed to generate planar electrodes on substrate surfaces. [19-21]

1.1.3 Conjugated Polymers

Conjugated polymers are characterized by distinctive electronic structures, featuring alternating single and double bonds along their backbone. This arrangement allows for the delocalization of π electrons, which leads to notable differences in their electronic and optical properties compared to traditional polymers.[22] While regular polymers tend to be insulators or have limited conductivity, conjugated polymers display semiconducting or metallic behavior, depending on their structure and doping level. This exceptional electronic behavior makes them highly appealing for various sensing applications.

They possess a heightened sensitivity to environmental changes, such as the presence of specific chemicals or variations in temperature and humidity.[19, 20, 22] Additionally, conjugated polymers can be designed or modified to interact with analytes or target

molecules selectively. This selectivity is crucial in sensing applications where the detection of specific substances or biomarkers is desired. [23, 24]

Conjugated polymers exhibit rapid response times due to their efficient charge transfer and transport properties. This enables them to swiftly detect and transmit signals in real-time, making them suitable for dynamic sensing applications. Moreover, conjugated polymers can be easily processed into various forms, such as thin films, nanoparticles, or composites, facilitating their integration into different sensing platforms and devices.[25]

Their versatility allows conjugated polymers to find applications in diverse fields, including chemical sensing, biosensing, environmental monitoring, and healthcare diagnostics.[26-28] Overall, the unique electronic properties, sensitivity, selectivity, fast response, and versatility of conjugated polymers make them highly attractive for sensing applications. They hold the potential to enhance detection capabilities and drive the development of more advanced sensing technologies.

1.1.3.1. Background, Synthesis, and Applications for Polyaniline (PANI)

PANI is a conducting polymer that has been extensively studied in electrochemical sensing due to its high conductivity, excellent chemical durability, environmental stability, simplicity of synthesis, and low cost.[29] It is frequently used as a film, which typically has great mechanical, electromagnetic, optical, and gas-sensing capabilities.[30, 31] An electrochemical technique or basic chemical oxidative polymerization can produce PANI.

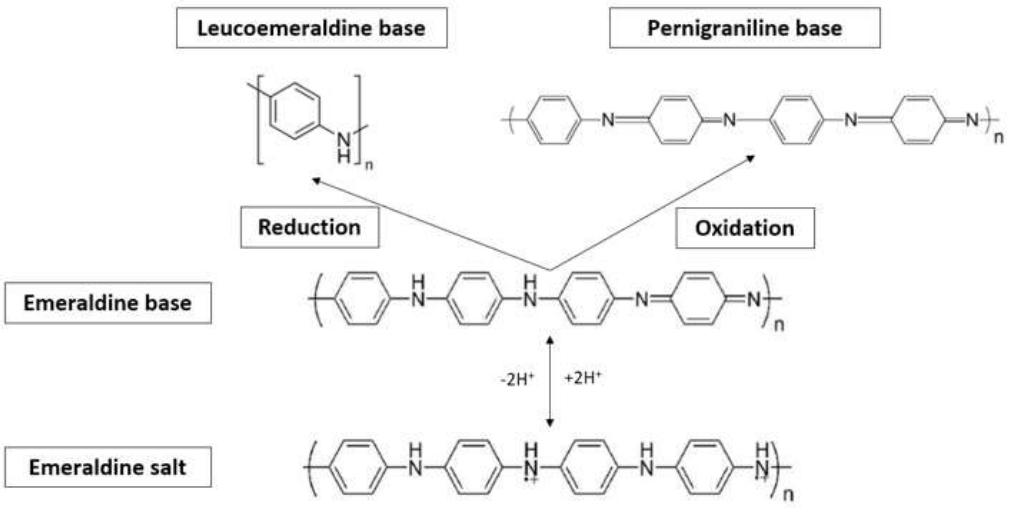

Figure 1 Oxidation states of PANI

The chemical structure of PANI has various oxidation states as salt or base. Leucoemeraldine is the reduced form of PANI, the half-oxidized state is called Emeraldine, and Pernigraniline is the fully oxidized state (Figure 1). [32] Emeraldine salt (ES) is the only conducting state of PANI out of all the states. The conducting emeraldine base can be transformed into the conducting emeraldine salt by doping with various protonic acids. The conductivity can be controlled by varying the doping amount, and the ES can be doped back to the insulating form via deprotonation using a base. The highly conducting form of PANI (ES) is regulated by two completely different processes: protonic acid doping and oxidative doping. [33, 34] These intrinsic redox reactions produce various electrical characteristics that vary easily with doping, making the material suitable for applications. Due to its remarkable qualities, PANI has prospective applications in various disciplines, including organic electronics, biomedical domains, and anti-corrosion materials.[35]

1.1.3.2. Background, Synthesis, and Applications for Polydiacetylene (PDA)

PDAs, characterized by a conjugated backbone with alternating single and triple carbon-carbon bonds, possess unique chromatic properties that make them well-suited for sensing applications.[36] External stimuli (e.g. organic solvents, pH) can induce a reduction in the effective conjugation length and a transition from low to high energy within the absorption spectrum. Consequently, this leads to the manifestation of optically red PDA, which has the potential to emit fluorescence [35, 36], which make them attractive for various sensing applications such as detection of volatile organic compounds[37], and thermochromic sensor[38]. Additionally, PDA polymers exhibit rapid response times, enabling real-time monitoring and quick detection of changes in the sensing environment.[39]

PDA undergoes a structural transformation during polymerisation that changes colour from colourless or pale to intense blue. Conformational change in the PDA structure with external stimuli solution can induce a colour change from blue to red, referred to as the red phase. This change occurs due to alterations in the conjugated π-electron system within the PDA backbone, leading to modifications in the absorption spectrum.[40]

Incorporating indifferent forms of PDA polymers, such as films, nanoparticles, or hydrogels, facilitates their integration into various sensor designs and platforms.[41, 42] The mechanisms and factors influencing the red shift in PDA may vary depending on the

particular PDA system and the applied external stimuli. However, understanding and utilizing the colour transitions in PDA provide valuable insights for developing sensors and smart materials used in chemical detection.

1.2 Sensor Fabrication

Miniaturized sensor fabrication employs various techniques to create small-sized sensors with high sensitivity and functionality. Some commonly used techniques for miniaturized sensor fabrication include microfabrication, MEMS, nanofabrication, thin film deposition and 3D printing. [43, 44] The choice of technique depends on the specific sensor requirements, target application, and desired performance characteristics.

Electrode-based sensor fabrication involves the creation of sensors that utilize electrodes as the key components for sensing and signal transduction. These sensors use the interaction between the analyte of interest and the electrodes to generate a measurable electrical signal. A substrate made of glass, silicon, or polymers is prepared as the base on which the electrodes can be deposited. The substrate should have suitable properties for electrode adhesion and stability.

Electrodes are deposited onto the substrate using different techniques. The choice of deposition method depends on factors such as electrode material, desired thickness, and pattern requirements. Electrode-based sensors can be used in various applications, such as chemical sensing, biosensing and gas sensing.[45, 46] The design and fabrication of electrode-based sensors require careful consideration of materials, electrode geometry, surface modifications, and signal transduction mechanisms to ensure optimal performance and sensitivity for the target analyte.[47, 48]

1.2.1 Electrode-based potentiometric pH sensors

Directly detecting electrochemical reactions using potentiometric electrochemical sensors offers a straightforward and appealing method for investigating samples. A typical potentiometric sensor combines two electrodes: a reference electrode and a sensitive (working) electrode. These sensors measure the open circuit potential between two electrodes immersed in solutions with varying pH levels, as indicated by the Nernst equation ($E=E^o - \frac{RT}{nF} \ln Q$).[49, 50]

Including the Ag/AgCl/KCl layer is essential in potentiometric pH sensors, specifically for reference electrodes. The development of the KCl layer plays a crucial role in ensuring the stability and reproducibility of data. Previous advancements have enabled the creation of miniaturized thick film reference electrodes utilizing polymer Ag/AgCl, glassy AgCl, glassy Ag/AgCl, and glass-KCl layers.[51] However, the inflexibility and instability associated with these designs pose significant challenges, particularly for wearable systems. Alternatively, implementing flexible reference electrodes using polymer substrates demonstrates exceptional performance with minimal potential variation, even when subjected to different bending states.[52] This innovation addresses the limitations of traditional designs and provides enhanced functionality. In parallel, the working electrode facilitates the monitoring of oxidation or reduction processes occurring close to its surface.

1.2.2 Electrode-based gas sensors

Despite increasingly complicated industrial processes, there is a growing need for gas sensors to detect environmentally toxic, hazardous, and volatile organic compounds. These sensors detect changes in electrical properties due to specific gases or vapors in the surrounding environment. The interaction between sensing materials and analytes at the chemical interface is critical in determining the sensor's performance. In gas sensors, the created sensors can gauge variations in frequency, capacitance, and impedance values.[53, 54] They offer advantages such as high sensitivity, selectivity, and real-time monitoring capabilities.

CHAPTER 2. Materials and Methods

2.1 Materials

Ammonium persulfate (APS), chloroform, polyethylene oxide (PEO), carbon black (CB), sodium dodecylbenzene sulphonate (SDBS), ferric chloride, nafion (5% in alcohol), hydrochloric acid (HCl, 0.1M, and 1M), aniline, tetrahydrofuran (THF), acetic acid, ammonium, methanol, and TRIS base were purchased from Merck. Commercial polyethylene terephthalate (PET) film was used as a polymer substrate.

2.2 Method

2.2.1 Polyaniline (PANI) Polymerization

Method 1

0.02 M SDBS (0.17 g) was dissolved in 25 ml of HCl (1 M) with stirring for 1 hour. 0.2 M aniline (460 µl) was added to this solution and stirred for 30 minutes. APS was dissolved in a round-bottomed balloon flask containing 25 ml of HCl (1 M) at a concentration of 0.25 M (1.42 g) and stirred under nitrogen, N_2 for 1 hour. APS solution was added dropwise to the aniline-containing solution for 1 hour and then sonicated in an ultrasonic bath for 3 minutes. The final solution was left to stir for 6 hours. During polymerization, the color of the solution changed from milky white to blue and then dark green. After this color change occurred, stirring was stopped, and the solution was left to rest. The next day, the PANI solution was filtered, washed first with water, then 20 ml of HCl (0.1 M), and finally methanol. PANI powder was dried in a vacuum at 80°C. [55-57]

Method 2

In this method, a surfactant was not employed in contrast to the first approach. The steps are summarized as follows:

First, 10 ml of 0.3 M aniline was dissolved in 80 ml of HCl (1 M) with stirring for 30 mins. The process was conducted in an ice bath to keep the temperature between 0 and 5°C. 0.3 M APS solution was prepared by mixing with 80 ml of HCl (1 M) in a separate beaker, and the APS solution was slowly added dropwise to the prepared aniline solution. This addition process took 1 hour and was still conducted in the ice bath at 0°C. After this process, the stirring was prolonged for another 5 hours to ensure the polymerization

reaction was complete. The colour of the resulting solution turned from white to dark green during the reaction. The next step involved keeping the solution overnight to allow for further reaction and formation of the polymer. Once the reaction was completed, the precipitates formed were separated by washing them several times with 1 M HCl and distilled water until the washing solution became colourless. Finally, the obtained polymer product was dried at a temperature of 70°C. Overall, the experiment involved the synthesis of a polymer from aniline using APS as the initiator under controlled temperature and continuous stirring. The final product was obtained after thorough washing and drying.[58]

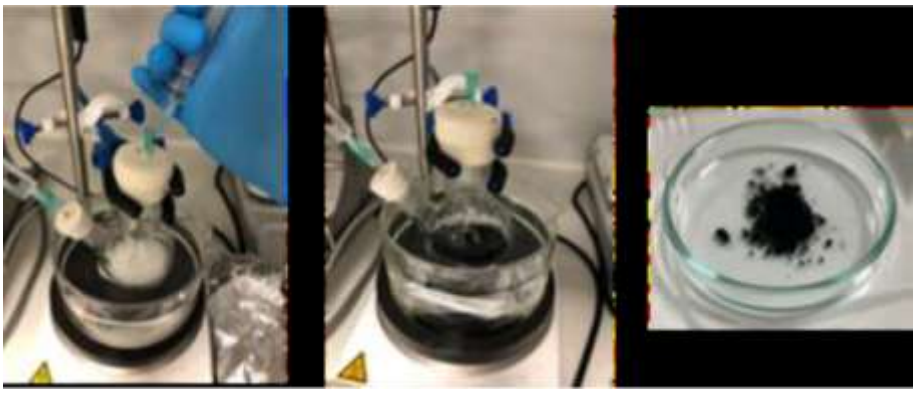

Figure 2 Synthesis of polyaniline

2.2.2 Characterization of PANI with FTIR and NMR Spectroscopy

Covalently bonded compounds absorb various electromagnetic radiation frequencies in the infrared spectrum. FTIR is an instrumental technique that uses the absorption of infrared radiation at a range of wavelengths to identify the functional groups in organic and inorganic substances. Shimadzu Affinity 1S FT-IR with a Pike GladiATR Technologies attenuated total reflectance (ATR) spectrometer was used to evaluate PANI in the 600 to 4000 cm^{-1} wavenumber range. The operation of FTIR-ATR revolves around the interaction between infrared light and the sample using total internal reflection. The sample is brought into contact with a high refractive index crystal in an ATR accessory such as diamond, germanium, or zinc selenide. When an infrared beam is directed at the crystal, it undergoes multiple internal reflections within the crystal.[59]

NMR spectroscopy is an instrumental technique that determines the atomic-level molecular structure of a material. All nuclei are electrically charged and have many spins. The external magnetic field makes energy transfer possible from lower to higher energy

levels. This energy transmission or absorption of energy causes a change in the spin of nuclei. Energy is released at the same frequency as the nuclei's spin returns to its starting point. This energy transfer corresponds to a signal, which is then processed to provide an identical signal in the related nucleus's NMR spectrum.[60] ^{1}H NMR spectra were recorded on a Bruker Avance Neo 700 spectrometer using deuterated dimethyl sulfoxide. (DMSO-d_6) at 298K. In this method, the location of H atoms in the chemical backbone of the PANI molecule synthesized was determined by the received signals.

2.2.3 Fabrication of Electrodes

The electron beam (e-beam) evaporation method is a physical vapor deposition process at relatively low substrate temperatures. In this process, an e-beam released from a tungsten filament strikes a target material placed inside a crucible and causes the atom to leave the material surface under a high vacuum. The evaporated target material coats everything in the vacuum chamber as the vaporized material precipitates into a solid form. [61] E-beam process offers extensive possibilities for controlling film structure and morphology with desirable properties such as dense coating, low contamination, high reliability, and high productivity. E-beam is accelerated to high kinetic energy and focused on the starting material. The kinetic energy of electrons is converted into thermal energy, which increases the surface temperature of the materials, causing evaporation and deposition on the substrate.[62] TORR International, Inc.'s e-beam evaporation instrument was used in this study. The evaporation method was preferred for planar electrode production because it provides a homogeneous coating.

2.2.3.1 Interdigitated Electrode (IDE) Design

The three critical parameters, including the spacing, G between the fingers, the width of each finger, W, and the number of fingers, N of interdigitated electrodes, were determined based on a previous study. [48, 63] A shadow mask has been produced via SolidWorks design to enable the production of interdigitated electrodes with various G, W, and N values. PET with a thickness of less than 250 μm was chosen as the substrate because of its excellent properties for flexible printed circuits. Before fabrication of the IDE, PET film was cleaned with isopropyl alcohol and then dried under nitrogen to ensure the substrate surface was free of defects and contamination. Silver, Ag slugs placed in a crucible were used as materials to be evaporated. The shadow mask adhered to the PET substrate, and both were placed in the e-beam evaporation system. The vapor deposition

chamber was reduced to 10^{-5} Torr pressure. 200 nm Ag was patterned through the shadow mask on a cleaned PET substrate. Only the designed IDE shown in Figure 3 is left when the shadow mask is removed from the substrate surface.

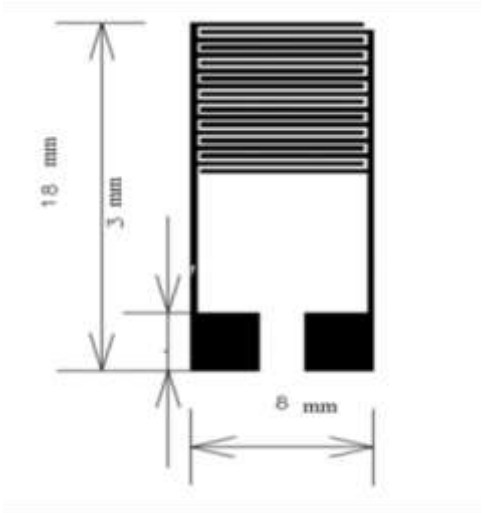

Figure 3 Schematic of an interdigitated electrode (IDE)

2.2.3.2 Potentiometric Electrode Design

Another electrode pattern was designed as one circular working electrode and one crescent-shaped reference electrode [64, 65] using the SolidWorks program with the given dimensions in Figure 4. The designed shadow mask was taped to the cleaned PET film on the metal plate. The metal plate was placed in the vacuum chamber. Using the e-beam evaporation method, 20 nm chromium, Cr and 200 nm Ag were deposited and patterned through the shadow mask on a cleaned PET substrate.

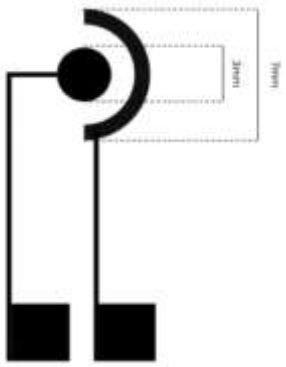

Figure 4 Schematic of a second pattern electrode for polyaniline sensor

2.2.4 Preparation of conjugated polymer

2.2.4.1 Preparation of conjugated polymer for gas sensing

The viscosity of the solution is one of the most important elements of the coating material. Therefore, a matrix polymer is added to increase the viscosity of polymer solutions. Based on our preliminary studies with various matrix polymers such as PVP, PEO, and PVA, PEO exhibited superior surface adhesion properties than others. Therefore, PEO was chosen as the matrix polymer in this research. 5% PEO solution and PDA solutions were prepared in chloroform. 500 µl PDA solution was mixed with 300 µl PEO solution, and the blend solution was sonicated for 20 minutes at room temperature. The prepared pink blend, PDA solution coats the electrode surface with the spin-coating method.

2.2.4.2 Preparation of conjugated polymer for pH sensing

10 mg PANI and 4 mg conductive carbon black (CB) were dissolved in 1 ml deionized water, DIW. Nafion was used as a matrix polymer to increase the viscosity and surface adhesion of the PANI/C solution. Nafion (5% in alcohol) was diluted to 2.5% Nafion with deionized water. 100 µl of 2.5% Nafion solution was added into 100 µl PANI/C solution.[66-68] The prepared PANI/C/Nafion solution was applied on the working electrode surface to create an active sensing surface for pH change detection.

2.2.5 Deposition of conjugated polymer coatings on pattern electrodes

2.2.5.1 Spin-coating of conjugated polymers

Spin coating is one of the advanced methods to produce thin and uniform film coating on the electrode surface. In this method, an excessive amount of solution is applied, and due to centrifugal forces, the liquid spreads homogeneously, and thus solidified film layer on the substrate by high spinning speed is obtained.[69] Since it has a simple and rapid procedure to produce uniform thin films to flat substrates, the interdigitated electrodes were coated with PDA polymer using spin-coating. In this application, the contact pads were covered with a paper to prevent contamination of the contact pads, important for further electronic characterization. A conductive band was used to hold this paper on the electrode. The electrode was placed on the sample holder, and the vacuum was turned on. 100 µL of the polymer blend was carefully poured dropwise onto the electrode with a syringe. The substrate is rotated at a speed of 2000 rpm for 40 seconds.

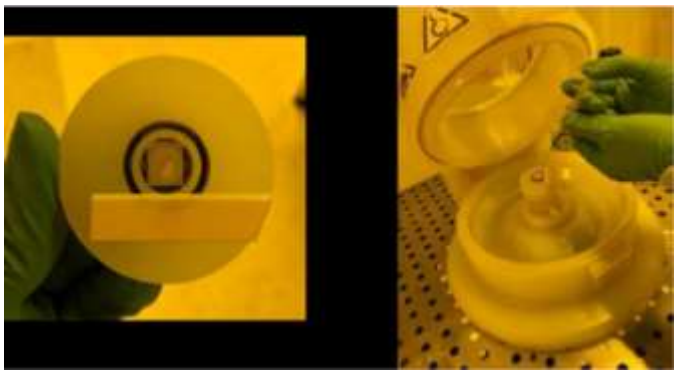

Figure 5 Spin-coating experimental setup

2.2.5.2 Drop-cast of Polyaniline (PANI)

The "drop casting" method, which is quick and simple, is frequently used to prepare the surface of chemically modified electrodes in which the modifying layer is composed of particles. In this procedure, a drop of liquid containing a suspension of the target particles is first applied to the electrode surface, and the particles of interest stay on the surface after the solvent evaporates. The designed working electrode was coated with the drop-cast method. To coat the working electrode, a 2.5 µL solution of PANI/C/Nafion was dropped onto the electrode surface, and it was subsequently dried in a fume hood at room temperature. (Figure 6. A-B).

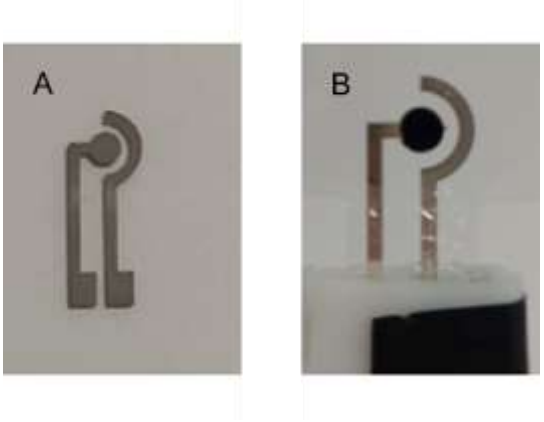

Figure 6 Uncoated (bare) electrode (A) and working electrode coated with PANI/C/Nafion coating (B)

2.2.6 Characterization of coating with optical microscopy and profilometer

Optical microscopy enlarges images of small materials using visible light and a set of lenses.[70] Before coating, an optical microscope (5X) was used to evaluate the bare electrode for cracks or merges between its silver fingers. After spin coating, the coating

was checked with the optical microscope (5X) again to confirm full surface coverage with the polymer blend (Figure 7).

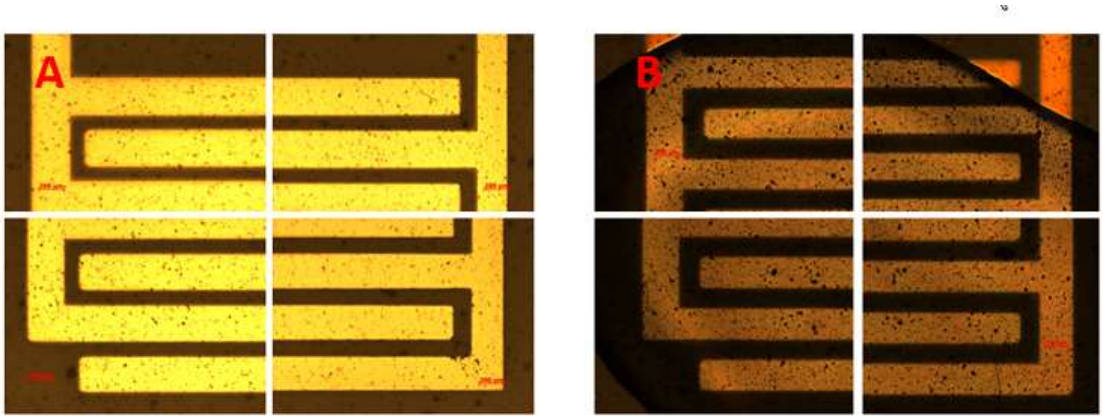

Figure 7 Optical microscope images of the bare electrode (A) and coated electrode (B).

Profilometer is an instrument used to characterize a coating's topographical feature. The sensitive stylus makes contact with the product substrate to distinguish the distinct features of a product substrate on nano-, and micro-scales.. [71] Profilometry is a simple method for determining film thickness on the substrate surface. The stylus moves from an uncoated substrate to a polymer-coated region to determine the step height and the polymer thickness. The coating thickness of the gas sensors was determined using a KLA Tencor Surface Profiler.

2.2.7 Sensor characterization

2.2.7.1 Sensor characterization and impedance measurement using an LCR meter

An LCR meter is a type of electronic instrument used to measure the inductance (L), capacitance (C), and resistance (R) of an electronic component. The LCR meter also measures the effective resistance of the sensor, known as the impedance. Impedance (Z) describes resistance to an AC-current's flow. It can be determined using the voltage V between the measurement target's terminals and the current flowing into the target.[72] In this study, the impedance of the prepared PDA-coated gas sensors was measured with a Hioki brand IM3523 LCR meter at 1 kHz and 1 V at room temperature. The sensor was first checked with a multimeter and then inserted into the adapter. The adapter was placed in the sealed box, and the LCR meter connection was made (Figure 8). In the LCR meter experimental setup, PDA-coated gas sensors were placed into the sealed box, and gases were introduced to the box.

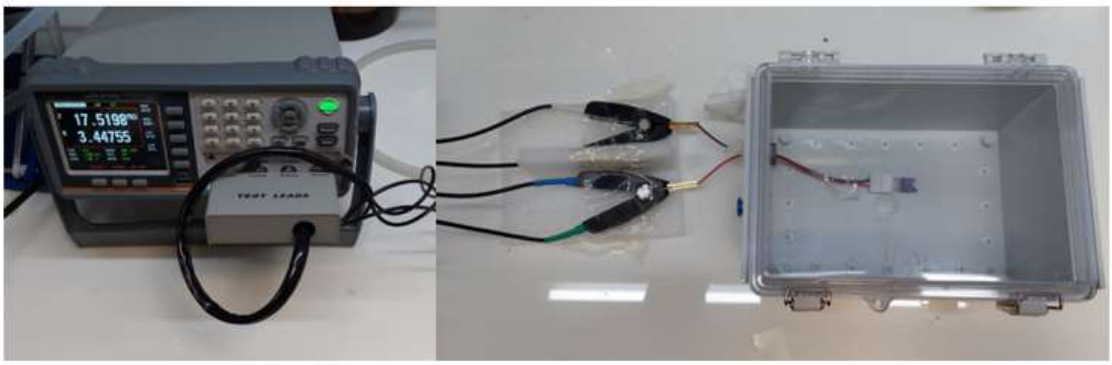

Figure 8 Gas sensor characterization setup connected to an LCR meter.

2.2.7.2 Gas exposure experiments

For acetic acid detection, N-(2-(Pentecost-10,12-diynoyloxy) amino) ethyl) ethane-1,2-diamine (PCDA-DETA) and N-(2-(tricosa-10,12-diynoyloxy) amino) ethyl) ethane-1,2-diamine (TCDA-DETA) coated electrodes were used. After the sensor had been installed in the sealed box and connected to the LCR meter, Acetic acid was introduced to the sealed box using a vapor delivery setup constructed consisting of a 15 cm glass bubbler, a mass flow controller (GMC1200, Atovac), and nitrogen gas (99.999 %). 10 mL of acetic acid (1 M, 99.9 %) was added to the glass bubbler, and the bubbler's output was connected to the sealed box. The vapor of the volatile liquid was directed to the PDA-coated electrode with the contribution of 200 sccm nitrogen as the carrier gas. Acetic acid was introduced to the electrode surface for 30 mins to trigger the color change from blue to red. After the sensor's color changed, acetic acid concentration was reduced with deionized water to determine the change in the impedance with respect to acetic acid concentration. In this process, 4 ml of the acetic acid solutions with different concentrations were poured into the tissue paper (7 cm x 7 cm), which was placed in a canister as a sample compartment and evaporated acetic acid from the surface of the tissue paper was carried to the sealed chamber with the help of 200 sccm nitrogen flow for 2.5 minutes. The impedance changes of sensors coated with PCDA-DETA and TCDA-DETA were evaluated with various acetic acid dilution by volume at 5%, 10%, 15%, 20%, 25%, 50%, 75%, and 100%.

The relationship between acetic acid concentration and vapor phase concentration was detected according to Raoult's Law. The vapor pressure of the acetic acid in the solution is proportional to its mole fraction in the solution. The vapor pressure is, therefore

$$PA = XA.P_0A \quad \text{Eq.1}$$

where,PA is the vapor pressure of acetic acid in solution, XA is the mole fraction of acetic acid in solution, and P_0A is the vapor pressure of pure acetic acid.

The vapor pressure of acetic acid is approximately 14.6 mmHg at 24 °C (temperature in the laboratory).

The vapor phase concentration can be calculated by

$$C = PA/Pa \quad \text{Eq.2}$$

where C is the concentration of acetic acid in vapor pressure, PA is the vapor pressure of acetic acid, and Pa is the atmospheric pressure. [73]

Following the formula, precise calculations were conducted to determine the exact proportions of water and acetic acid necessary for achieving target concentrations of 500 ppm. Consequently, a 2 ml solution was prepared by blending water and acetic acid in 8% v/v for 500 ppm. The prepared sensors coated with PCDA-DETA were tested using 100% water, 100% acetic acid, and an 8% acetic acid/water mixture (500 ppm). The 2 ml solutions were transferred into a sealed box in a petri dish. The samples were allowed to equilibrate until a stable impedance value was attained, as measured using an LCR meter. This procedure facilitated assessing the sensor's response to acetic acid vapor in the ambient environment, enabling the characterization of its performance in terms of parts per million (ppm).

2.2.7.3 Potentiostat

A potentiostat is an electronic device that detects the potential difference between a reference electrode and a working electrode. The electrochemical reaction in a cell occurs on the working electrode surface. The working electrode's potential change is measured using a reference electrode with a constant electrochemical potential (if there is no current). Potentiometric sensors are suitable for real-time measurement of pH change sensing. Therefore, the potentiometric sensor was designed with two different half-cells as one circular working electrode and one crescent-shaped reference on the substrate surface. The open circuit potential of the pH sensor was measured using PARSTAT MC-1000 potentiostat. Different pH buffers were used as electrolytes to connect the half-cells (RE and WE). The electrochemical reaction took place in a PANI-coated working

electrode. Various potential differences between the working electrode and the reference electrode were recorded depending on the mobility of the ions on the PANI surface with the application of buffers of different pH values on the PANI sensing film.

2.2.7.4 pH Measurement Experiment

The open circuit potential change of pH sensors was measured in different pH TRIS buffer solutions (pH 5, 6, 7, 8, 9). The TRIS buffer system was prepared as follows:

0.02 M Tris base was prepared in 300 mL of Milli Q water (18.5 MΩ·cm). 726.84 mg of Tris base (MW=121.14 g/mol) was dissolved in 200 mL Milli Q water. After dissolving the base in water, the volume was increased to 300 mL using Milli Q water. The pH of this stock solution 0.02 M Tris base was 9.1 at 23 °C. To prepare 50 mL of 0.01 M solution of desired pH range, 25 mL of 0.02 M stock solution was taken and then adjusted the pH with 0.1 M HCl. The solution volume was increased to 50 mL with Milli Q water when the desired pH was achieved.

In this process, sensors were connected to a potentiostat, and 100 µl of TRIS buffer (as an electrolyte) was applied to cover the working surface and reference electrodes. Because of the ionic movement, open circuit potential change was observed in different pH.

CHAPTER 3. Results and Discussion

3.1 PANI synthesis and characterization

In this thesis research, we developed a flexible pH sensor with PANI/C/Nafion active coating to monitor real-time pH levels. For this purpose, two distinct PANI syntheses were performed, one utilizing a surfactant (Method 1) and the other without the surfactant (Method 2). The conductivity of the PANI powders, prepared using two distinct methods, was evaluated using a multimeter. The measurements indicated that the PANI synthesized with surfactant (Method 1) exhibited significantly lower conductivity. This might be due to a disruption caused by surfactants during the formation of well-organized structures within the PANI matrix. Since these organized structures are crucial for facilitating effective charge transport and high conductivity, they might cause lower conductivity once disrupted.

Consequently, PANI was synthesized without surfactant (Method 2) with enhanced conductivity as the active coating of the working electrode. However, PANI synthesized through this method exhibited a pH value of 2. During the experiments, due to the corrosive nature of acid, the acidic PANI caused delamination on the silver surface. Therefore, the active coating preparations proceeded with PANI synthesized via Method 1. Carbon nanoparticles were included as an additive to the coating formula to compensate for the low conductivity of PANI.

Characterization of synthesized PANI was done by recording FTIR and 1H NMR spectra. As shown in the FTIR spectrum (Figure 9), 1630 cm^{-1} and 1520 cm^{-1} peaks are associated with the C = N and C = C strain vibrations of the quinone and benzene rings, respectively. The bands at 1358 cm^{-1} and 1194 cm^{-1} are bands of C-N and C=N strain vibrations. Vibrations of in-plane and out-of-plane C-H bending modes were detected at 845 cm^{-1}. The broad band at 3281 cm^{-1} is the tension band of the N-H bond. FTIR spectrum indicated the anticipated peaks associated with the PANI polymer, confirming the successful synthesis.[57]

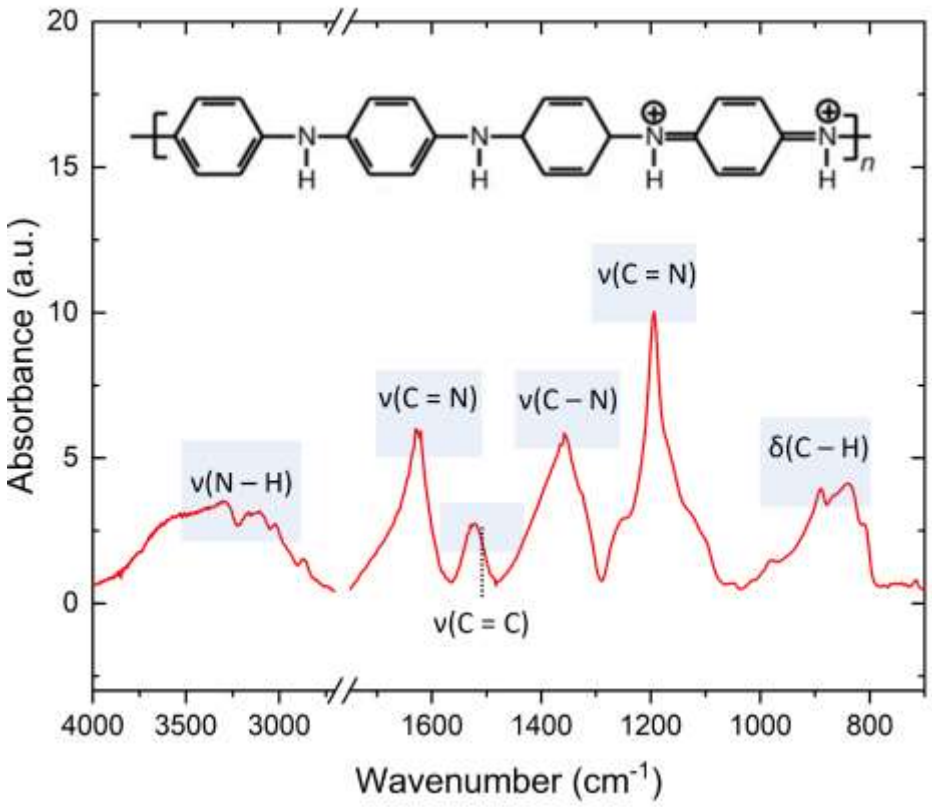

Figure 9 FT-IR spectrum of PANI-ES

The ^{1}H NMR spectrum of PANI-ES dissolved in DMSO-d6 is depicted in Figure 10. The chemical shift at 3.40 ppm indicated the presence of HOD originating from DMSO-d6, while the chemical shift at 2.50 ppm was attributed to the residual solvent DMSO-d6. Notably, the NMR spectrum of PANI exhibited three distinct sharp singlets at 7.082, 7.185, and 7.286 ppm, which can be attributed to 1H coupled to 14N, thereby confirming the protonated state (NH^{+}) of the PANI backbone. Furthermore, three doublets observed at 7.33, 7.36, and 7.46 ppm corresponded to the proton peaks originating from the CH groups in the benzenoid and quinoid rings. The presence of the secondary amine (NH) peak in PANI was inferred as the cause for the observed peaks at 8.1 ppm and 9.3 ppm. Notably, despite utilizing DMSO-d6 as the solvent, the detection of amine protons, which are typically not discernible in solution due to their rapid exchange with solvent protons, was made possible in Figure 10. The gradual exchange of NH protons with the solvent facilitated their visualization in the spectrum. Peaks within the 5.8 to 6 ppm range were attributed to terminal NH and NH_2 groups attached to a benzene ring. Moreover, a signal around 1 ppm suggested the presence of water molecules with terminal amine groups attached. [74]

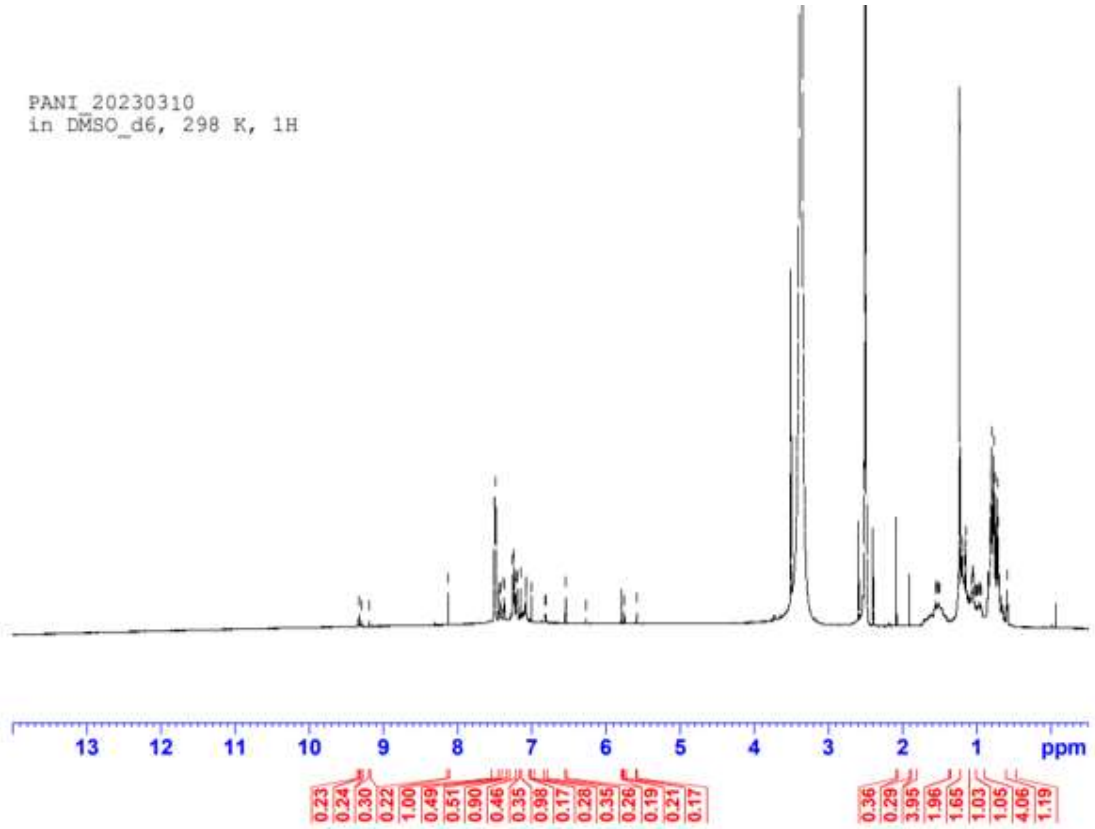

Figure 10 ^{1}H NMR spectrum of PANI-ES

3.2 Development and optimization of PANI-based pH sensor

In the fabrication process of electrochemical pH sensors, the initial step involved the design of patterned electrodes comprising working and reference electrodes constructed from silver. Inkjet printing, screen printing, and e-beam evaporation created a conductive surface on PET substrates. Compared to the e-beam method, inkjet printing and screen-printing offer the advantages of easier application, faster processing, and the ability to incorporate diverse electrode designs. However, it has been observed that electrodes produced through inkjet printing and screen-printing are not suitable for solution-based surface coating methods such as spin coating and drop-cast due to delamination issues on the electrode surface. Therefore, the e-beam method is chosen to produce the electrochemical sensors. PANI/C/Nafion blend was directly deposited onto the patterned Ag working electrode surface using the drop-casting technique to fabricate the pH sensor. Nafion matrix polymer was used to increase the adhesion of PANI/C coatings to the electrode surface. Moreover, Nafion is a cation exchanger resin that selectively allows protons through its surface, which improves the pH-sensing properties of the fabricated coating. [66, 75] In light of this knowledge, an initial investigation was conducted to examine the interactions between nafion and TRIS buffer specifically. In this study, the

working electrode surface was exclusively coated with nafion polymer, and open circuit potential measurements were recorded for 100 seconds using a potentiometer for each pH value.

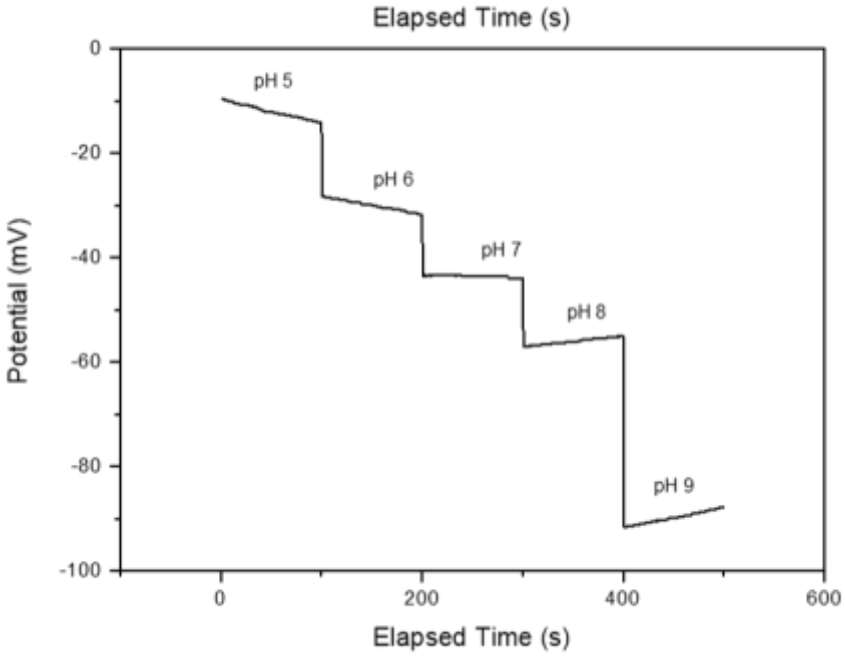

Figure 11 Open Circuit Potential Analysis of Nafion-Coated Electrode

The graphical representation in Figure 11 displays the relationship between Potential (mV) and Elapsed Time (s), illustrating the response of nafion when subjected to TRIS buffer solutions within the pH range of 5-9. Based on the obtained results, it was observed that the steps' difference within the pH range of 5 to 8 remained relatively constant at approximately 14 mV. However, a considerable shift of 37 mV was observed at pH 9. Since the ionic sites in the nafion membranes can be restructured as the hydration is increased, the efficient transport of the ions through the polymer membrane results in a prominent shift of the potential value at pH 9.[76] The presence of a potential difference in nafion-coated sensors can be attributed to the formation of a semipermeable membrane on the electrode surface. The protons (H^+) in the TRIS solution can pass through the nafion membrane. This permeability changes the proton concentration near the electrode surface and positively charged H+ particles affect the measured OCP. However, it has been noted that the differences in potential observed at different pH values are lower than in previous studies [49, 50, 77, 78] on pH sensors, indicating that using nafion as a matrix polymer does not pose any obstacles.[50, 77, 78] Furthermore, the proton permeability

property of nafion is considered a supportive element for the pH sensor, contributing to its overall effectiveness.[79] Ensuring the inclusion of a conductive coating is essential alongside using a proton-permeable matrix polymer to enhance the sensor's ability to detect changes in ion concentrations or pH. In this context, the introduction of conductive CB was employed to enhance the conductivity of the PANI polymer significantly. Therefore, pH sensors were fabricated with working electrodes coated with PANI/C/Nafion.

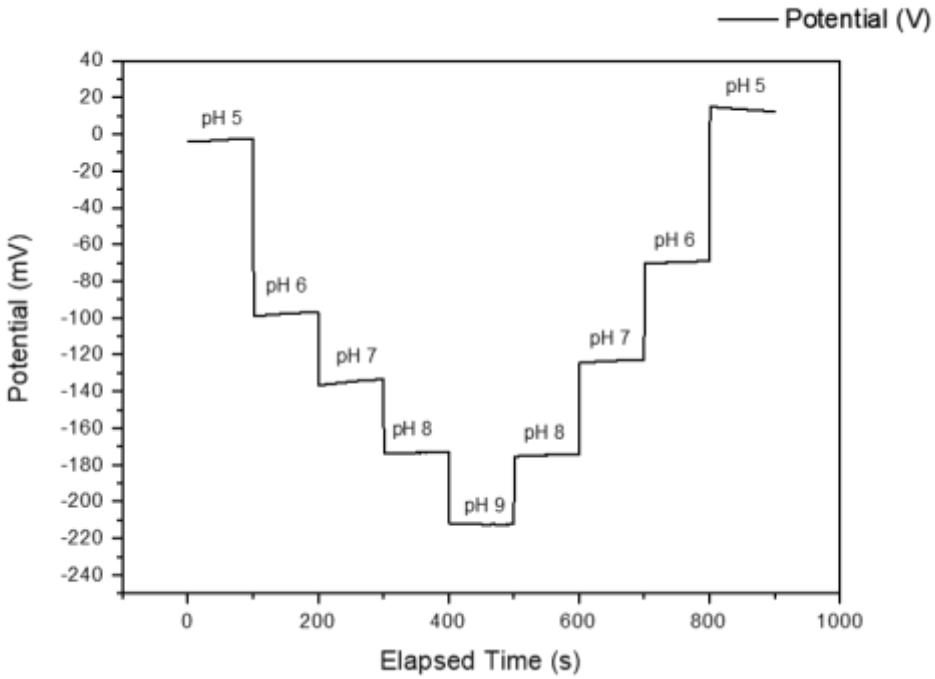

Figure 12 Open Circuit Potential Measurements of the PANI/C/Nafion coated electrode at pH 5-9 and reversibility testing of the sensor

The performance of the fabricated pH sensors was assessed by measuring the potential difference between the reference electrode and the working electrode for each pH value within the pH range of 5-9, as illustrated in the graph presented in Figure 12. 100-second data acquisition intervals were employed for each TRIS buffer solution pH value. Throughout the 100-second measurement intervals, each pH value exhibited a consistent and constant potential difference. Distinct changes in the recorded potential difference values were observed for each pH value, resulting in a step-like pattern. The observed open circuit potential measured at pH 5 was about -3 mV, whereas, at pH 6, it significantly decreased to -99 mV. The measurements revealed an approximate 96 mV open circuit potential change. However, as the pH values increased, the potential difference decreased

to approximately 40 mV. Furthermore, when the sensor was measured in the reverse direction from pH 9 to pH 5, it displayed similar potential differences with the forward direction from pH 5 to pH 9, indicating the reversibility of the sensor. Despite the similarity, there is a slight variation in potential differences for pH 5 and 6. When the pH is measured from 5 to 9 and then 9 to 5, the response for pH 5 and 6 is not similar due to the hysteresis effect observed in sensing devices.[75] The deviation of response might be caused by the loss of sensitivity of the PANI/C/Nafion coating because its deprotonation is faster than protonation. The variation in results observed with the PANI coating at different pH levels can be attributed to the pH-induced fluctuations occurring across the entire surface of the PANI sensing coating. The contact between the coating and electrolytes possessing distinct pH values causes changes in the sensor's resistance, subsequently leading to potential differences between the working electrode and reference electrode. A step-like plot in the potential is attributed to the distinct and discrete changes occurring in the proton [H^+] of the measured system. Whenever there is a sudden shift in pH, it triggers a rapid and immediate adjustment in the potential. This abrupt transition is visually represented as a well-defined step in the plot, and the step-like behavior emerges due to the system's heightened sensitivity to alterations in pH. [80, 81]

The Nernst equation is a fundamental equation used to describe the relationship between the concentration of a species and the electrode potential. In the case of a pH sensor, the Nernst equation can be used to relate the change in pH to the change in electrode potential. The Nernst equation for a pH electrode is given by:

$$E = E^0 + (RT/nF) * \ln([H^+]) \quad \text{Eq.3}$$

Where: E is the electrode potential E^0 is the standard electrode potential, R is the ideal gas constant, T is the temperature in Kelvin, n is the number of electrons transferred in the half-reaction, F is Faraday's constant, and [H^+] is the concentration of hydrogen ions (protons). [82]

Assuming a standard hydrogen electrode as the reference electrode and considering room temperature (approximately 298 K), the Nernst equation for a pH electrode simplifies to:

$$E = E^0 + (0.0592/n) * pH \quad \text{Eq.4}$$

In this equation, the factor of 0.0592/n represents the Nernstian slope, which is the change in potential per pH unit. At room temperature, with a single electron transfer (n = 1), the Nernstian slope is approximately 0.0592 V/pH or 59 mV/pH. This value of 59 mV per pH unit is widely accepted as the Nernstian response for a pH sensor at room temperature, and it is commonly used in the design and calibration of pH electrodes. [83]

In the current study, the results showed low Nernstian values of 40 mV showing the involvement of an unequal number of electrons and protons coupled to deprotonation reactions [84, 85]. Several factors can affect the sensitivity and, therefore, the sub-Nernstian behavior of the fabricated sensor, such as molecules with the surfactant during PANI synthesis.[86] The presence of SDBS molecules in the synthesis process led to the formation of micelles with the aniline monomer molecules. This interaction resulted in a decrease in the availability of the aniline monomers for binding within the growing polymer chain. Additionally, the micelle formation played a role in maintaining separation between the polymer chains.[87] As a consequence, the interchain interactions between the polymer chains colud be reduced. Consequently, these effects can cause a decrease in the sensitivity of the polyaniline (PANI) layer to changes in pH, leading to the generation of sub-Nernstian signals.

3.3 Production and Evaluation of Impedimetric Gas Sensor Utilizing PCDA-DETA Conjugated Polymer

The conjugated polymer, PCDA-DETA, was used as the active sensing component of the coating applied on the IDEs PCDA-DETA via spin coating to produce impedimetric gas sensors.

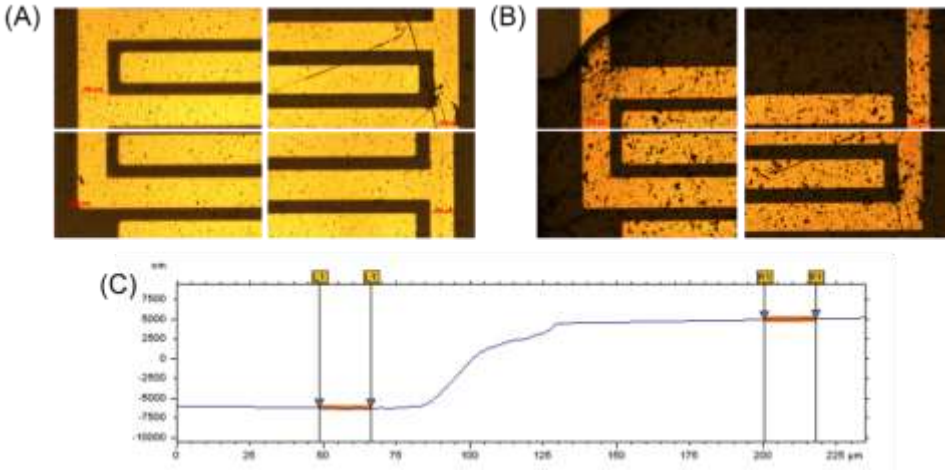

Figure 13 Uncoated IDE (A), PCDA-DETA coated IDE (B) and profilometer plot (C)

The viscosity of the PCDA-DETA monomer solution was improved by adding PEO as the matrix polymer in the coating formula. In this way, a homogeneous coating of approximately ~11 micrometres (Figure 13. C) thickness was obtained. The optical microscopy images of the uncoated and coated IDE surfaces are shown in Figure 13 (A-B). The image shows the coating of PCDA-DETA extending uniformly across all IDE fingers, confirming the homogenous coating.

After the PCDA-DETA monomer was coated on the IDE surface, it was photopolymerized under UV exposure (254 nm) for 10 minutes. The sensitivity of the poly(PCDA-DETA), which possesses polyamines as the head group, to acetic acid vapor was tested by performing impedance measurements. The blue phase poly(PCDA-DETA) transitions to the red phase under external stimuli, in this case, under exposure to acetic acid vapor. The changes in impedance were recorded during the acetic acid vapor exposure. Figure 14 shows an almost steady impedance of around 14 Mohm for 400 seconds while in the blue phase. The impedance value dropped suddenly from ~ 14 Mohm to 5 Mohm after transforming from the blue phase to the red phase. Then, a gradual increase in impedance was observed for an extended time of ~ 4000 secs, reaching ~ 13.6 Mohm.

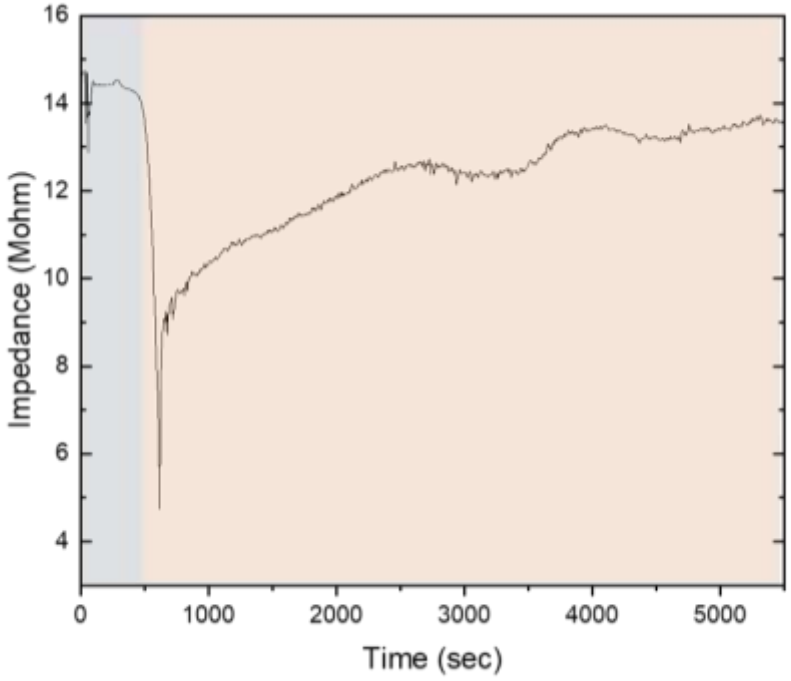

Figure 14 Impedance measurement of poly(PCDA-DETA) during the blue-to-red phase transition

The impedance measurement in Figure 14 illustrates the poly(PCDA-DETA) transformation from the blue phase to the red phase over time following its interaction with acetic acid. Upon the poly(PCDA-DETA) transformation from the blue phase to the red phase, the impedance value exhibited a sudden decline from approximately 14.4 Mohm to 5 Mohm. Following this decrease, there was a gradual increase, reaching an approximate value of 13.6 Mohm. This change in impedance value is that the secondary bonds between the substitutional amine group were broken, and it caused a conformational change in polymer structure to compensate for this strain from blue to red phase transition.[88] The conformational change in the molecular structure of poly(PCDA-DETA) induces alterations in the electrical properties of the polymer. These changes in electrical properties generate detectable signals, allowing for the measurement and analysis of poly(PCDA-DETA)'s electrical response.

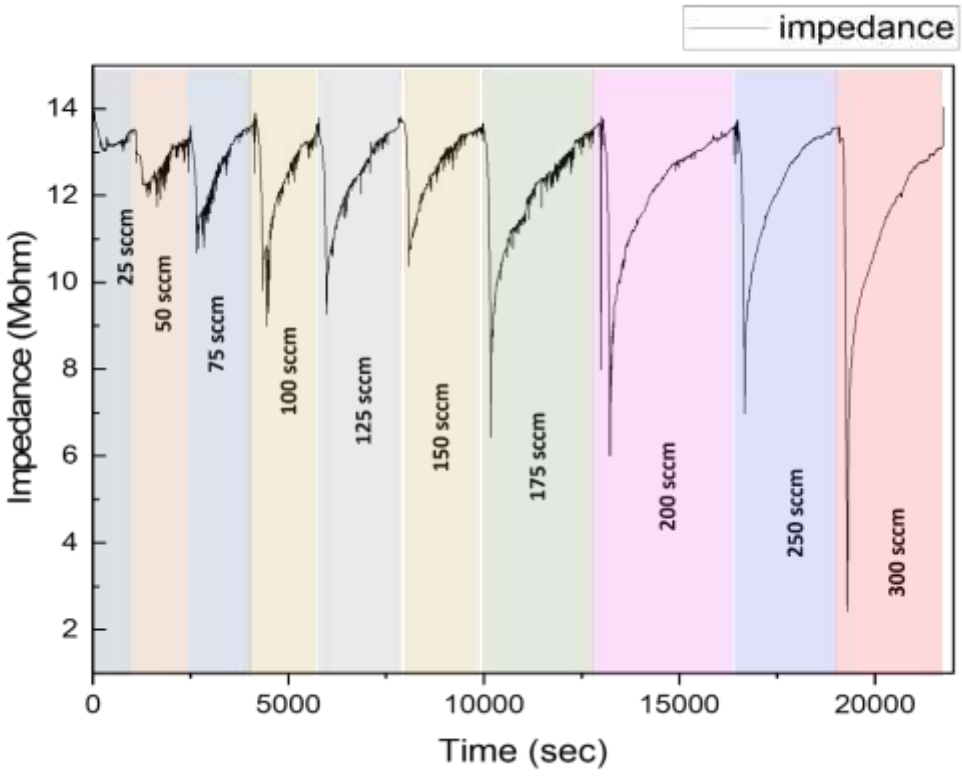

Figure 15 The impedimetric response of poly(PCDA-DETA) through varied acetic acid introduction rates

Such a sudden drop in impedance might be due to breaking the H-bonds between amine groups leading to the conformational change in the polymer backbone. A change in the backbone conformation of poly(PCDA-DETA) alters the electrical properties of the

polymer. The red phase poly(PCDA-DETA)-PEO coated sensors were exposed to various nitrogen flow rates. Nitrogen acts as the carrier gas for the acetic acid vapor generated in the bubbler. The sensor's impedance changes were recorded while increasing the nitrogen flow rate from 25 sccm to 300 sccm. Figure 15 shows the impedance trends of the sensor with an initial drop, followed by the recovery after each exposure. The starting impedance value is ~ 13.5 Mohm. The impedance drops to lower values when the flow rate increases. At 50 sccm flow rate, the impedance change is only 1.5 Mohm, whereas the change is 11.5 Mohm at 300 sccm. This observed behavior suggests that the interaction between acetic acid molecules and the amine groups on the film surface facilitates a conformational change, reducing impedance. Therefore, more acetic acid molecules interacting with the surface induce a greater drop in the impedance signal within a defined time period. The sensor gradually reverts to its initial impedance value of ~ 13.5 Mohm upon the termination of acetic acid vapour exposure.

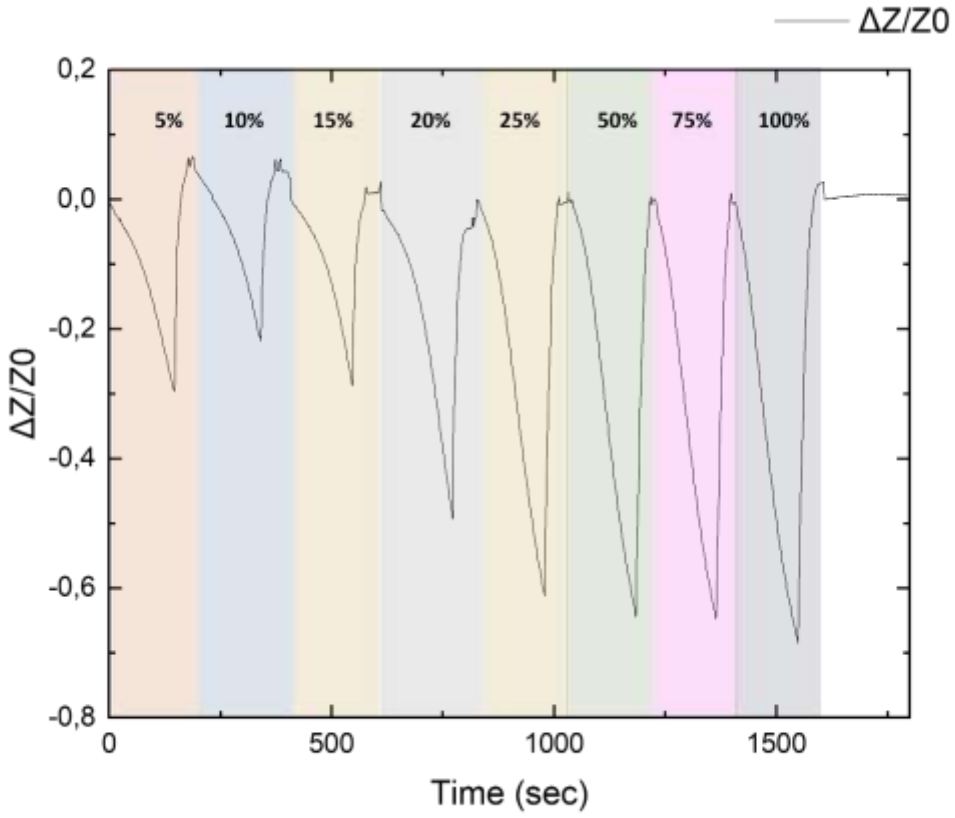

Figure 16 The impedimetric response of poly(PCDA-DETA) coated sensor to water-acetic acid solutions with varied ratios

Figure 16 illustrates the electrical response of the gas sensors in an enclosed chamber after being exposed to various acetic acid concentrations for 150 seconds. In this experiment, pure acetic acid was diluted with DI water to a total volume of 4 ml to make different acetic acid concentrations by volume (5% - 100%). The sensor's response to acetic acid vapor was evaluated at room temperature using the same gas setup equipped with a bubbler. The adsorbed acetic acid on the sensor surface was eliminated by introducing inert N_2 gas for 150 seconds to recover the sensor's impedance value to its baseline. This observation indicates that the acetic acid molecules form temporary interaction with the sensing layer, and the interaction can be removed quickly with inert N_2 gas. The assessment of sensors that did not revert to their initial impedance values within the given recovery period was conducted by comparing each measurement's initial and final impedance values. In this case, the impedance measurements were evaluated with the following formula according to the change between each measurement's first and last values.

$$\frac{\boldsymbol{Z-Z0}}{\boldsymbol{Z0}} = \frac{\boldsymbol{\Delta Z}}{\boldsymbol{Z0}} \qquad \text{Eq.5}$$

where Z0= first impedance value before acetic acid application, Z= impedance value after acetic acid application. According to this formula, the $\frac{\boldsymbol{\Delta Z}}{\boldsymbol{Z0}}$ = 0 means that there is no response, and when the $\frac{\boldsymbol{\Delta Z}}{\boldsymbol{Z0}}$ = -1, is equivalent to maximum response.

As a result, introducing acetic acid within the 5% to 15% concentration range resulted in an impedance change of -0.2. At the 20% acetic acid concentration, the impedance change was -0.5. For concentrations ranging between 25% and 75%, the impedance change was approximately -0.6. Lastly, 100% acetic acid caused an impedance change of -0.7. Despite the poor resolution to identify each concentration distinctively, it is observed that the relative impedance change increases as the acetic acid concentration increases.

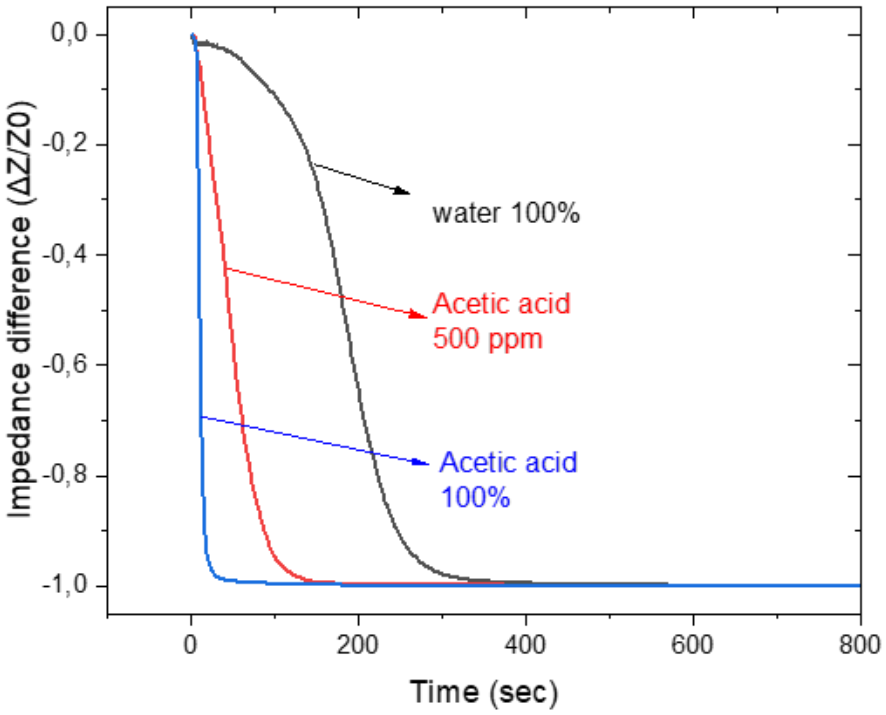

Figure 17 Response of poly(PCDA-DETA) to 100% water and 100% acetic acid

In Figure 17, the impedance change in the sensor was evaluated by comparing its performance in 100% water, 500 ppm acetic acid, and 100% acetic acid vapors in an unlimited time interval. In this experiment, the impact of the water utilized for dilution on the obtained results was examined. Following this analysis, despite the reaction rates being slowest in water and fastest in 100% acetic acid, it was determined that the impedance changes reached a similar level after 400 sec. The results indicate that while the acetic acid sensor demonstrates efficacy in short measurement durations, its selectivity to detect acetic acid diminishes over extended measurement periods. The results indicate the sensor exhibits poor resolution in distinguishing different acetic acid concentrations. This poor resolution can be attributed to two main factors: the sensor's response to sensing binary liquids, specifically water vapor and acetic acid vapor, and the impact of prolonged measurement on its performance.

A second sensor was manufactured utilizing the drop-cast method with PCDA-DETA, omitting the use of a matrix polymer, PEO, in the sensing layer formula. The exclusion of the PEO matrix polymer in the production of the second sensor is attributed to the concern that the hygroscopic nature of PEO, a polymer known to absorb and retain moisture, could potentially induce alterations in the physical properties of its coating.[89] Consequently, the presence of moisture retained by PEO may not only fail to influence

the electrode surface and its impedance but also compromise the desired performance of the sensor.

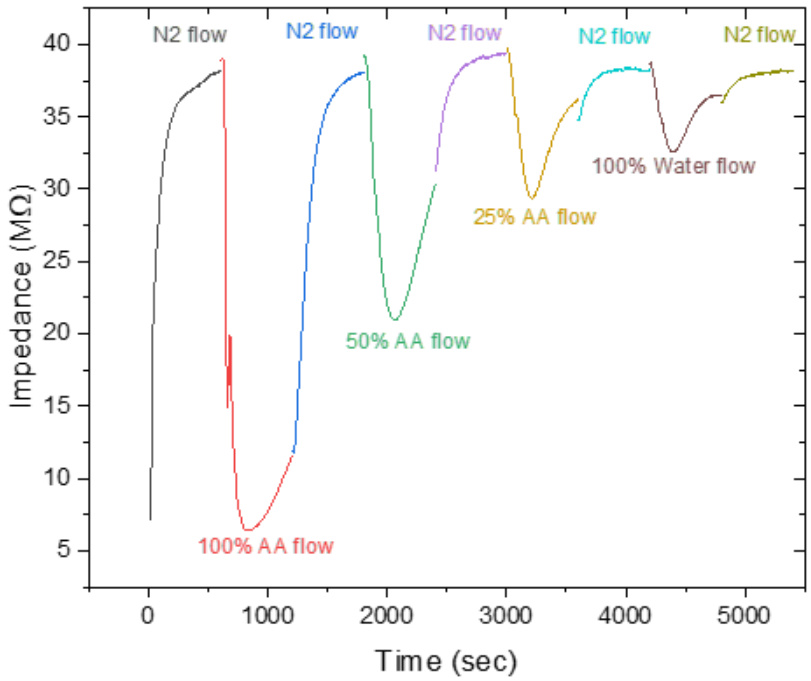

Figure 18 Impedance characterization of poly(PCDA-DETA) coated electrodes in response to varying concentrations of acetic acid.

The sensors were subjected to vapor-containing concentrations of 100%, 50%, and 25% acetic acid and 100% water (Figure 18). Upon introducing N_2 gas to return to its baseline value of 37 Mohms. The use of N_2 gas is to eliminate the acetic acid adsorbed by the sensor's surface. The original impedance value was restored through 10 minutes of N_2 purging at each experiment cycle, effectively reducing the recovery time. In the subsequent trials involving 50% and 25% acetic acid concentrations, the impedance values were measured and determined to be 21 Mohm and 29 Mohm, respectively. The effect of the water solution used for dilution on the sensor was examined in a control experiment where pure water resulted in an impedance value of 33 Mohms. This outcome suggests that water can potentially enhance surface conductivity and consequently contribute to changes in impedance. However, the results indicate a decrease in acetic acid concentration within the solution corresponds to reduced impedance values. It has been observed that the sensor possesses selectivity towards acetic acid and can be utilized for detecting acetic acid, given its heightened response to this particular substance.

3.4 Production and Evaluation of Impedimetric Gas Sensor Utilizing TCDA-DETA Conjugated Polymer

TCDA-DETA differs from the PCDA-DETA with a shorter alkyl tail length. It possesses 23 Carbons, whereas PCDA has 25 carbons. The shorter alkyl tail length causes weaker dispersion forces between diacetylene monomers. In this study, by replacing poly(PCDA-DETA) with poly(TCDA-DETA), the sensor's response, thereby, the sensitivity to acetic acid, is evaluated. The active coating was prepared by mixing TCDA-DETA monomer solution with the matrix polymer, PEO, to attain the desired viscosity for homogenous coating. The coating on IDE was evaluated from the optical microscopy images shown in Figure 19. A-B. The images confirmed a uniform and consistent surface coating. The thickness of the coating was measured as ~12 micrometers with a profilometer (Figure 19. C).

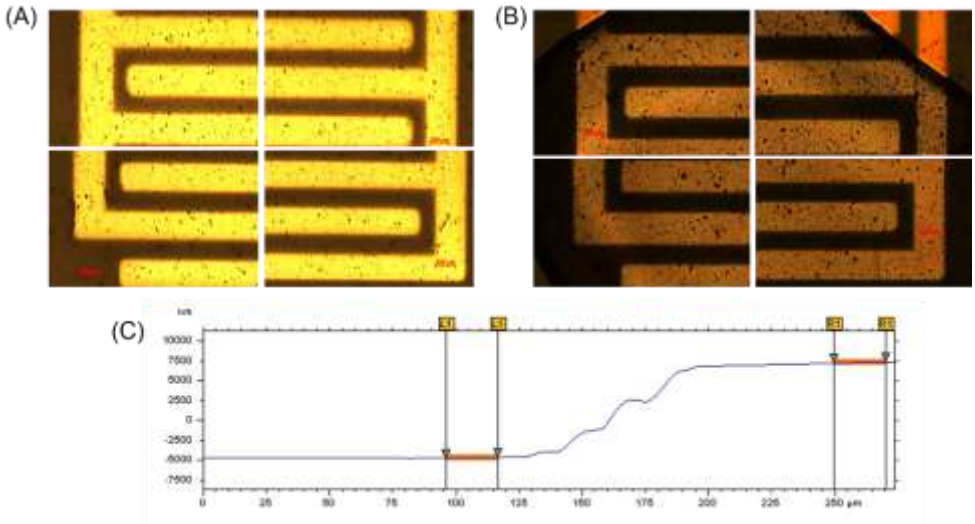

Figure 19 Uncoated IDE (A), TCDA-DETA coated IDE (B) and profilometer graph (C)

After applying the TCDA-DETA monomer onto the IDE surface, it was subjected to UV exposure at a wavelength of 254 nm for 10 minutes to initiate photopolymerization. The sensitivity of the resulting poly(TCDA-DETA), which incorporates polyamines as the head group, to acetic acid vapor was evaluated through impedance measurements. The poly(TCDA-DETA) material exhibits a blue phase, which transitions to a red phase when exposed to acetic acid vapor. During the exposure to acetic acid vapor, changes in impedance were recorded to assess the sensor's response.

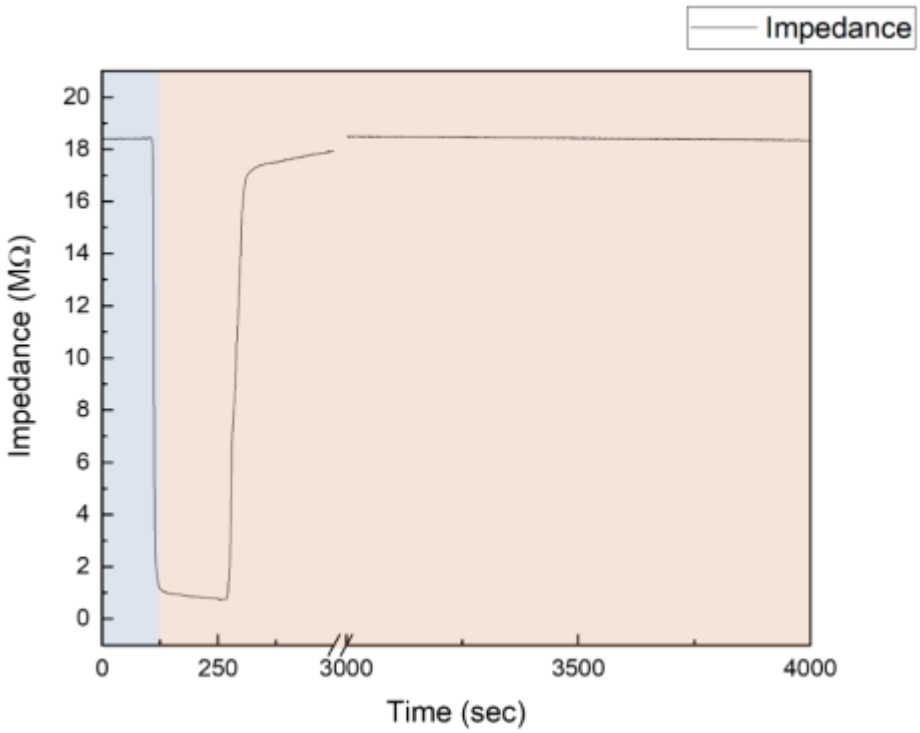

Figure 20 Impedance measurement of poly(TCDA-DETA) during the blue-to-red phase transition

In Figure 20, the impedance remains relatively constant at approximately 18.5 Mohm for approximately 100 seconds while the sensor is in the blue phase. Subsequently, there is a sudden drop in impedance from around 18.5 Mohm to 0.8 Mohm upon the transformation from the blue phase to the red phase. Following this transition, the impedance gradually increases over an extended period of approximately 4000 seconds, eventually reaching a value of approximately 18.5 Mohm. The observation revealed that sensors coated with poly(PCDA-DETA) required approximately 400 seconds to transition from the blue phase to the red phase, whereas sensors coated with Poly(TCDA-DETA) accomplished this transition in approximately 100 seconds. This clear difference in transition time indicates that poly(TCDA-DETA) is more sensitive to acetic acid vapor than poly(PCDA-DETA). The difference in sensitivity between poly(TCDA-DETA) and poly(PCDA-DETA) can be attributed to the structural properties of the TCDA-DETA monomers. Specifically, the TCDA-DETA monomers have shorter alkyl end groups compared to PCDA-DETA. As a result, the poly(TCDA-DETA) material experiences weaker dispersion forces within its structure. [90] The weaker dispersion forces in poly(TCDA-DETA) allow for faster conformational changes in response to acetic acid vapor. [91]This means that when exposed to acetic acid, the poly(TCDA-DETA) coating undergoes a

more rapid transition from the blue phase to the red phase compared to poly(PCDA-DETA) coatings. Thus, the poly(TCDA-DETA) coated sensors exhibit higher sensitivity to acetic acid due to the faster conformational change facilitated by shorter alkyl end groups in the TCDA-DETA monomers.[91]

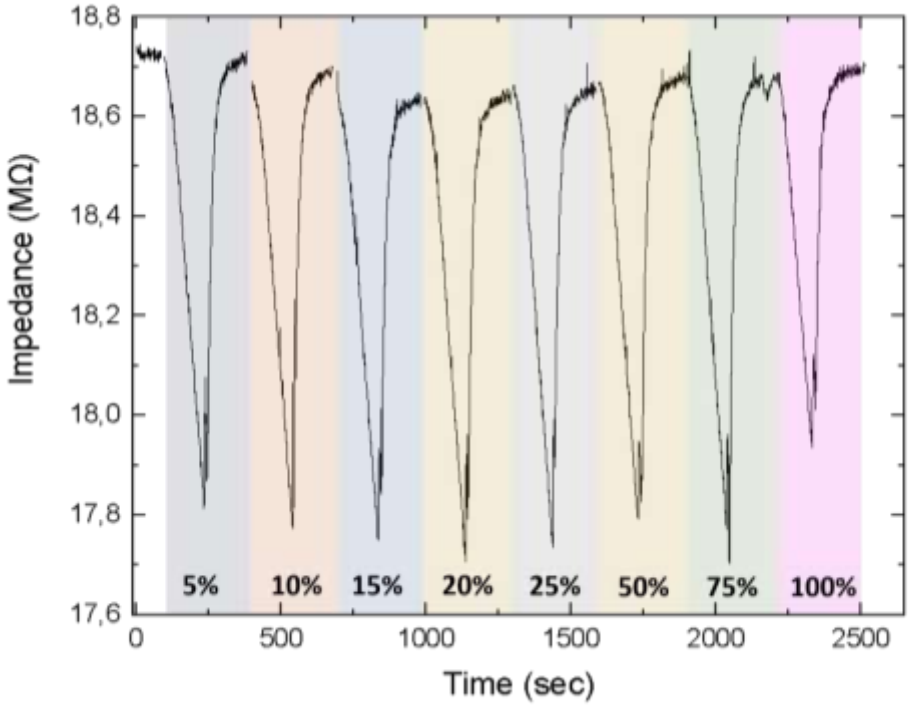

Figure 21 The impedimetric response of poly(TCDA-DETA) coated sensor to water-acetic acid solutions with varied ratios

IDE coated with poly(TCDA-DETA)-PEO was exposed to acetic acid vapor diluted with water ranging from 5 % to 100 % for 150 seconds. Nitrogen was introduced for 150 seconds to remove residual acetic acid from the sensor surface and accelerate recovery. Figure 21 shows the impedance change at each exposure with different acetic acid dilution ratios. Results showed similar impedance change values from 18.7 Mohm to 17.8 Mohm, with ~ 1 Mohm change at each exposure. Even though the sensor was exposed to different amounts of acetic acid concentrations, the response did not change accordingly. The response from the poly(PCDA-DETA)-PEO coated IDE system differed due to shorter alkyl chains in the TCDA-DETA structure. These shorter alkyl chains lead to weaker dispersion forces, resulting in a surface exhibiting heightened sensitivity towards acetic acid. Consequently, the increased sensitivity masks the differences between concentrations, making it challenging to observe distinct variations.

CHAPTER 4. CONCLUSIONS

Conjugated polymer-coated electrode-based flexible sensors combine the unique properties of conjugated polymers with the flexibility and versatility of electrode-based platforms, enabling the development of lightweight, conformable, and wearable sensing devices. The conjugated polymer deposited on a 2-probe patterned electrode acts as the sensing element, interacting with the target analyte to induce changes in its electrical properties.

Several types of flexible sensors were developed with several conjugated polymers, including PANI, PDA and its derivatives. We showed that PANI conjugated polymer coated on an Ag working electrode surface could operate as an electrochemical pH sensor. A composite material consisting of PANI, carbon and nafion is formulated for the sensing layer to address several challenges of the sensor development, including adhesion, conductivity, and proton transfer. Incorporating a matrix polymer, nafion not only improves the adhesion of PANI onto the surface effectively but also facilitates proton conduction due to the high density of sulfonic acid groups along its polymer backbone.

OCP measurements were performed using a potentiostat to assess and characterize the performance of the PANI/C/Nafion sensor. The measurements made from pH 5 to 9 recorded that OCP was almost constant at each pH value for 100 seconds of measurement. However, a sudden decrease in OCP was observed when the measurement started with the next pH solution, and a step-like graph occurred. Based on the open circuit potential, it was observed that the potential difference between steps registered as approximately 40 mV. These findings conclusively establish the sensor's sensitivity towards variations in pH levels. Additionally, measuring the sensor in the opposite direction from pH 9 to pH 5 exhibited comparable potential differences to those observed in the forward direction from pH 5 to pH 9. This observation indicates that the sensor demonstrates reversibility, maintaining consistent behavior regardless of the pH direction. Following the Nernst equation, a discrepancy of approximately 59 mV was expected between the steps depicted in the measurement graphs. However, it was determined upon examination that the actual value between pH 6-9 was approximately 40 mV. The underlying cause for this phenomenon is believed to stem from a reduced interaction of monomer molecules during PANI synthesis, potentially attributable to the presence of a surfactant.

Future investigations could focus on exploring diverse synthesis methods for PANI, aiming to eliminate the incorporation of surfactants.

It is well-established that PCDA-DETA and TCDA-DETA conjugated polymers exhibit a colorimetric response to acid groups originating from the amine head groups in their molecular backbones. Following the initial polymerization, the conjugated polymers transition to the blue phase, and upon exposure to acid, they transform to the red phase due to the disruption of hydrogen bonds in the head groups and the consequent alteration of polymer alignment. Instead of monitoring the colorimetric response of the responsive polymer upon exposure to a trigger like an acetic acid vapour, this study focuses on developing conjugated polymer sensors to observe the corresponding electrical response of these polymers. The impedance measurements confirm that the impedance value of PCDA-DETA and TCDA-DETA polymers decreases upon exposure to acetic acid vapor. Furthermore, the impedance value returns to its original state once the acetic acid exposure is terminated or when the N_2 gas is purged. Unlike the irreversible colorimetric response from the blue-to-red phase, the observed electrical response demonstrates reversibility and reusability of the sensors fabricated using these PDA polymers. Upon acetic acid vapour exposure, the blue-to-red transition corresponds to a single sharp impedance decrease that could only recover to a different impedance value over time when acetic acid vapour is cut off. Therefore, we determined that the red phase impedance value differs from the blue phase vesicles. Interestingly, the red phase PDA vesicles are responsive to acetic acid vapour, as shown with the reversible impedance measurement for various acetic acid vapour concentrations.

Additionally, it has been observed that these sensors exhibit a prompt response to acetic acid, with detection occurring within approximately 100 seconds. However, the ambient humidity affected the sensitivity of the sensors produced using the PEO (polyethylene oxide) matrix polymer employed for spin coating application. Consequently, sensor fabrication continued without the matrix polymer and instead employed a drop-casting method. PCDA-DETA-coated sensors exhibited varied responses to different concentrations of acetic acid at distinct rates, while TCDA-DETA-coated sensors displayed similar responses across the concentration range. This disparity can be attributed to the shorter alkyl chain in TCDA-DETA, rendering it more sensitive to all gasses. Consequently, this study found PCDA-DETA-coated IDE sensors more suitable for acetic acid detection than TCDA-DETA sensors.

In conclusion, two flexible electrode-based sensors were developed in this thesis study. The interaction between target analytes and the conjugated polymers in these sensors induced modifications in the electrical response sensed via the patterned conductive surfaces. This distinctive behavior enabled the detection of specific analytes within a given medium. It has been determined that the potential difference between the reference and working electrodes changes for different pH values of PANI-based electrochemical sensors. In addition, experimental measurements have proven that PDA-coated IDE electrodes can detect various acetic acid concentrations in the gas phase. These sensors have significant potential to detect target particles in various applications in the food and healthcare industries.

CHAPTER 5. REFERENCES

[1] Y. Zhang *et al.*, "Flexible nanohybrid microelectrode based on carbon fiber wrapped by gold nanoparticles decorated nitrogen doped carbon nanotube arrays: In situ electrochemical detection in live cancer cells," *Biosensors and Bioelectronics*, vol. 100, pp. 453-461, 2018.

[2] B. K. Dadhich, B. Panda, M. S. Sidhu, and K. P. Singh, "Nanodiamonds enable femtosecond-processed ultrathin glass as a hybrid quantum sensor," *Scientific Reports*, vol. 13, no. 1, p. 6286, 2023.

[3] D. Arora, P. Kumar, S. Singh, A. Goswami, and D. Kaur, "Flexible magnetoelectric sensor and nonvolatile memory based on magnetization-graded Ni/FSMA/PMN-PT multiferroic heterostructure," *Applied Physics Letters*, vol. 122, no. 26, 2023.

[4] H. Malik *et al.*, "Algal-based wood as a green and sustainable alternative for environmentally friendly & flexible electronic devices membrane bioreactor," *Chemosphere*, p. 139213, 2023.

[5] J. Zhou *et al.*, "Flexible and wearable acoustic wave technologies," *Applied Physics Reviews*, vol. 10, no. 2, 2023.

[6] E. Smecca *et al.*, "AlN texturing and piezoelectricity on flexible substrates for sensor applications," *Applied Physics Letters*, vol. 106, no. 23, 2015.

[7] Q.-H. Lu and F. Zheng, "Polyimides for electronic applications," in *Advanced Polyimide Materials*: Elsevier, 2018, pp. 195-255.

[8] R. Nisticò, "Polyethylene terephthalate (PET) in the packaging industry," *Polymer Testing*, vol. 90, p. 106707, 2020.

[9] D. Vilela, A. Romeo, and S. Sánchez, "Flexible sensors for biomedical technology," *Lab on a Chip*, vol. 16, no. 3, pp. 402-408, 2016.

[10] M. Akiyama *et al.*, "Flexible piezoelectric pressure sensors using oriented aluminum nitride thin films prepared on polyethylene terephthalate films," *Journal of Applied Physics*, vol. 100, no. 11, 2006, doi: 10.1063/1.2401312.

[11] A. Bafaqeer, M. Tahir, and N. A. S. Amin, "Synthesis of hierarchical ZnV2O6 nanosheets with enhanced activity and stability for visible light driven CO2 reduction to solar fuels," *Applied Surface Science*, vol. 435, pp. 953-962, 2018/03/30/ 2018, doi: https://doi.org/10.1016/j.apsusc.2017.11.116.

[12] B.-Y. Chang and S.-M. Park, "Electrochemical impedance spectroscopy," *Annual Review of Analytical Chemistry*, vol. 3, pp. 207-229, 2010.

[13] A. Mortari, A. Maaroof, D. Martin, and M. B. Cortie, "Mesoporous gold electrodes for sensors based on electrochemical double layer capacitance," *Sensors and Actuators B: Chemical*, vol. 123, no. 1, pp. 262-268, 2007.

[14] N. O. Laschuk, E. B. Easton, and O. V. Zenkina, "Reducing the resistance for the use of electrochemical impedance spectroscopy analysis in materials chemistry," *RSC advances*, vol. 11, no. 45, pp. 27925-27936, 2021.

[15] C. Thirstrup and L. Deleebeeck, "Review on Electrolytic Conductivity Sensors," *IEEE Transactions on Instrumentation and Measurement*, vol. 70, pp. 1-22, 2021, doi: 10.1109/TIM.2021.3083562.

[16] J. R. Stetter, W. R. Penrose, and S. Yao, "Sensors, chemical sensors, electrochemical sensors, and ECS," *Journal of The Electrochemical Society*, vol. 150, no. 2, p. S11, 2003.

[17] W. Göpel, "Chemical imaging: I. Concepts and visions for electronic and bioelectronic noses," *Sensors and Actuators B: Chemical,* vol. 52, no. 1-2, pp. 125-142, 1998.
[18] M. J. McGrath, C. N. Scanaill, M. J. McGrath, and C. N. Scanaill, "Sensing and sensor fundamentals," *Sensor technologies: Healthcare, wellness, and environmental applications,* pp. 15-50, 2013.
[19] W. Qiu *et al.*, "An electron beam evaporated TiO 2 layer for high efficiency planar perovskite solar cells on flexible polyethylene terephthalate substrates," *Journal of Materials Chemistry A,* vol. 3, no. 45, pp. 22824-22829, 2015.
[20] F. Molina-Lopez, D. Briand, and N. De Rooij, "All additive inkjet printed humidity sensors on plastic substrate," *Sensors and Actuators B: Chemical,* vol. 166, pp. 212-222, 2012.
[21] E. P. Randviir, D. A. Brownson, J. P. Metters, R. O. Kadara, and C. E. Banks, "The fabrication, characterisation and electrochemical investigation of screen-printed graphene electrodes," *Physical Chemistry Chemical Physics,* vol. 16, no. 10, pp. 4598-4611, 2014.
[22] T. Mikie *et al.*, "Extended π-electron delocalization in quinoid-based conjugated polymers boosts intrachain charge carrier transport," *Chemistry of Materials,* vol. 33, no. 21, pp. 8183-8193, 2021.
[23] G. Anantha-Iyengar *et al.*, "Functionalized conjugated polymers for sensing and molecular imprinting applications," *Progress in Polymer Science,* vol. 88, pp. 1-129, 2019.
[24] L. Feng, C. Zhu, H. Yuan, L. Liu, F. Lv, and S. Wang, "Conjugated polymer nanoparticles: preparation, properties, functionalization and biological applications," *Chemical Society Reviews,* vol. 42, no. 16, pp. 6620-6633, 2013.
[25] G. Kaur, R. Adhikari, P. Cass, M. Bown, and P. Gunatillake, "Electrically conductive polymers and composites for biomedical applications," *Rsc Advances,* vol. 5, no. 47, pp. 37553-37567, 2015.
[26] J. Yao, M. Yang, and Y. Duan, "Chemistry, biology, and medicine of fluorescent nanomaterials and related systems: new insights into biosensing, bioimaging, genomics, diagnostics, and therapy," *Chemical reviews,* vol. 114, no. 12, pp. 6130-6178, 2014.
[27] E. T. da Silva, D. E. Souto, J. T. Barragan, J. de F. Giarola, A. C. de Moraes, and L. T. Kubota, "Electrochemical biosensors in point-of-care devices: recent advances and future trends," *ChemElectroChem,* vol. 4, no. 4, pp. 778-794, 2017.
[28] F. Lv, T. Qiu, L. Liu, J. Ying, and S. Wang, "Recent advances in conjugated polymer materials for disease diagnosis," *Small,* vol. 12, no. 6, pp. 696-705, 2016.
[29] C. Awuzie, "Conducting polymers," *Materials Today: Proceedings,* vol. 4, no. 4, pp. 5721-5726, 2017.
[30] K. Phukan, S. Chutia, G. P. Chutia, and N. Sen Sarma, "Fabrication of Conducting Polyaniline–Betel Nut Fiber Filaments with Potential Ammonia Gas Sensing Behavior," *Journal of Natural Fibers,* vol. 19, no. 16, pp. 13694-13710, 2022.
[31] N. Y. Elamin, A. Modwi, W. Abd El-Fattah, and A. Rajeh, "Synthesis and structural of Fe3O4 magnetic nanoparticles and its effect on the structural optical, and magnetic properties of novel Poly (methyl methacrylate)/Polyaniline composite for electromagnetic and optical applications," *Optical Materials,* vol. 135, p. 113323, 2023.
[32] J. E. de Albuquerque, L. H. C. Mattoso, R. M. Faria, J. G. Masters, and A. G. MacDiarmid, "Study of the interconversion of polyaniline oxidation states by

optical absorption spectroscopy," *Synthetic Metals*, vol. 146, no. 1, pp. 1-10, 2004/10/14/ 2004, doi: https://doi.org/10.1016/j.synthmet.2004.05.019.
[33] A. H. Majeed *et al.*, "A Review on polyaniline: Synthesis, properties, nanocomposites, and electrochemical applications," *International Journal of Polymer Science*, vol. 2022, 2022.
[34] L. Tamayo, H. Palza, J. Bejarano, and P. A. Zapata, "8 - Polymer Composites With Metal Nanoparticles: Synthesis, Properties, and Applications," in *Polymer Composites with Functionalized Nanoparticles*, K. Pielichowski and T. M. Majka Eds.: Elsevier, 2019, pp. 249-286.
[35] M. Beygisangchin, S. Abdul Rashid, S. Shafie, A. R. Sadrolhosseini, and H. N. Lim, "Preparations, properties, and applications of polyaniline and polyaniline thin films—A review," *Polymers*, vol. 13, no. 12, p. 2003, 2021.
[36] C. Kim, C. Hong, and K. Lee, "Structures and strategies for enhanced sensitivity of polydiacetylene(PDA) based biosensor platforms," *Biosensors and Bioelectronics*, vol. 181, p. 113120, 2021/06/01/ 2021, doi: https://doi.org/10.1016/j.bios.2021.113120.
[37] H. Jiang, Y. Wang, Q. Ye, G. Zou, W. Su, and Q. Zhang, "Polydiacetylene-based colorimetric sensor microarray for volatile organic compounds," *Sensors and Actuators B: Chemical*, vol. 143, no. 2, pp. 789-794, 2010.
[38] O. Mapazi, P. K. Matabola, R. M. Moutloali, and C. J. Ngila, "A urea-modified polydiacetylene-based high temperature reversible thermochromic sensor: Characterisation and evaluation of properties as a function of temperature," *Sensors and Actuators B: Chemical*, vol. 252, pp. 671-679, 2017.
[39] B. Yoon, S. Lee, and J.-M. Kim, "Recent conceptual and technological advances in polydiacetylene-based supramolecular chemosensors," *Chemical Society Reviews*, vol. 38, no. 7, pp. 1958-1968, 2009.
[40] H. Shin, "The Colorimetric and Fluorescent Sensors Based on Heterocycle Containing Polydiacetylene (PDA)," 한양대학교, 2021.
[41] Y. Wu, H. Wang, F. Gao, Z. Xu, F. Dai, and W. Liu, "An injectable supramolecular polymer nanocomposite hydrogel for prevention of breast cancer recurrence with theranostic and mammoplastic functions," *Advanced Functional Materials*, vol. 28, no. 21, p. 1801000, 2018.
[42] C. He, Z. Feng, S. Shan, M. Wang, X. Chen, and G. Zou, "Highly enantioselective photo-polymerization enhanced by chiral nanoparticles and in situ photopatterning of chirality," *Nature Communications*, vol. 11, no. 1, p. 1188, 2020.
[43] A. S. Algamili *et al.*, "A review of actuation and sensing mechanisms in MEMS-based sensor devices," *Nanoscale research letters*, vol. 16, pp. 1-21, 2021.
[44] A. Tricoli, N. Nasiri, and S. De, "Wearable and miniaturized sensor technologies for personalized and preventive medicine," *Advanced Functional Materials*, vol. 27, no. 15, p. 1605271, 2017.
[45] R. Pradhan *et al.*, "Optimization, fabrication, and characterization of four electrode-based sensors for blood impedance measurement," *Biomedical Microdevices*, vol. 23, pp. 1-9, 2021.
[46] Z. Yu, Y. Tang, G. Cai, R. Ren, and D. Tang, "Paper electrode-based flexible pressure sensor for point-of-care immunoassay with digital multimeter," *Analytical chemistry*, vol. 91, no. 2, pp. 1222-1226, 2018.
[47] M. Ibrahim, J. Claudel, D. Kourtiche, and M. Nadi, "Geometric parameters optimization of planar interdigitated electrodes for bioimpedance spectroscopy," *Journal of Electrical Bioimpedance*, vol. 4, no. 1, pp. 13-22, 2013.

[48] A. Bourjilat, F. Sarry, D. Kourtiche, and M. Nadi, "Modelization of interdigitated electrode sensor for impedance spectroscopy measurement," in *2017 Eleventh International Conference on Sensing Technology (ICST)*, 2017: IEEE, pp. 1-5.
[49] L. Manjakkal, K. Zaraska, K. Cvejin, J. Kulawik, and D. Szwagierczak, "Potentiometric RuO2–Ta2O5 pH sensors fabricated using thick film and LTCC technologies," *Talanta*, vol. 147, pp. 233-240, 2016.
[50] L. Manjakkal, D. Szwagierczak, and R. Dahiya, "Metal oxides based electrochemical pH sensors: Current progress and future perspectives," *Progress in Materials Science*, vol. 109, p. 100635, 2020.
[51] L. Manjakkal, C. L. Pascual, and R. Dahiya, "Electrochemical sensors with screen printed Ag| AgCl| KCl reference electrodes," in *2017 IEEE SENSORS*, 2017: IEEE, pp. 1-3.
[52] J. Sun *et al.*, "A novel flexible Ag/AgCl quasi-reference electrode based on silver nanowires toward ultracomfortable electrophysiology and sensitive electrochemical glucose detection," *Journal of Materials Research and Technology*, vol. 9, no. 6, pp. 13425-13433, 2020.
[53] C. B. A. Hassine, H. Kahri, and H. Barhoumi, "A novel impedimetric sensor based on CuO (NPs)/polyaniline/murexide composite for cholesterol detection," *Journal of the Iranian Chemical Society*, pp. 1-9, 2022.
[54] G. Behzadi Pour and L. Fekri Aval, "Monitoring of hydrogen concentration using capacitive nanosensor in a 1% H2–N2 mixture," *Micro & Nano Letters*, vol. 13, no. 2, pp. 149-153, 2018.
[55] T. Jeevananda, J. H. Lee, and Siddaramaiah, "Preparation of polyaniline nanostructures using sodium dodecylsulphate," *Materials Letters*, vol. 62, no. 24, pp. 3995-3998, 2008/09/15/ 2008, doi: https://doi.org/10.1016/j.matlet.2008.05.041.
[56] P. T. Patil, R. S. Anwane, and S. B. Kondawar, "Development of Electrospun Polyaniline/ZnO Composite Nanofibers for LPG Sensing," *Procedia Materials Science*, vol. 10, pp. 195-204, 2015/01/01/ 2015, doi: https://doi.org/10.1016/j.mspro.2015.06.041.
[57] I. Sapurina, A. Riede, and J. Stejskal, "In-situ polymerized polyaniline films: 3. Film formation," *Synthetic Metals*, vol. 123, no. 3, pp. 503-507, 2001/09/24/ 2001, doi: https://doi.org/10.1016/S0379-6779(01)00349-6.
[58] I. Gawri, S. Khatta, K. P. Singh, and S. K. Tripathi, "Synthesis and characterization of polyaniline as emeraldine salt," *AIP Conference Proceedings*, vol. 1728, no. 1, 2016, doi: 10.1063/1.4946338.
[59] A. A. Ismail, F. R. van de Voort, and J. Sedman, "Chapter 4 Fourier transform infrared spectroscopy: Principles and applications," in *Techniques and Instrumentation in Analytical Chemistry*, vol. 18, J. R. J. Paré and J. M. R. Bélanger Eds.: Elsevier, 1997, pp. 93-139.
[60] R. R. Ernst, G. Bodenhausen, A. Wokaun, and A. G. Redfield, "Principles of Nuclear Magnetic Resonance in One and Two Dimensions," *Physics Today*, vol. 42, no. 7, pp. 75-76, 1989, doi: 10.1063/1.2811094.
[61] T. Kerdcharoen and C. Wongchoosuk, "11 - Carbon nanotube and metal oxide hybrid materials for gas sensing," in *Semiconductor Gas Sensors*, R. Jaaniso and O. K. Tan Eds.: Woodhead Publishing, 2013, pp. 386-407.
[62] P. Sun, X. Li, J. Shao, and P. V. Braun, "High-Performance Packaged 3D Lithium-Ion Microbatteries Fabricated Using Imprint Lithography," *Advanced Materials*, https://doi.org/10.1002/adma.202006229 vol. 33, no. 1, p. 2006229, 2021/01/01 2021, doi: https://doi.org/10.1002/adma.202006229.

[63] M. Ibrahim, J. Claudel, D. Kourtiche, and M. Nadi, "Geometric parameters optimization of planar interdigitated electrodes for bioimpedance spectroscopy," *Journal of Electrical Bioimpedance*, vol. 4, no. 1, pp. 13-22, 3913, doi: doi:10.5617/jeb.304.

[64] Q. Bao *et al.*, "Printed flexible bifunctional electrochemical urea-pH sensor based on multiwalled carbon nanotube/polyaniline electronic ink," *Journal of Materials Science: Materials in Electronics*, vol. 30, no. 2, pp. 1751-1759, 2019/01/01 2019, doi: 10.1007/s10854-018-0447-5.

[65] S. Mahinnezhad *et al.*, "Fully Printed pH Sensor Based in Carbon Black/Polyaniline Nanocomposite," in *2021 IEEE Sensors*, 31 Oct.-3 Nov. 2021 2021, pp. 1-4, doi: 10.1109/SENSORS47087.2021.9639597.

[66] S. Chinnathambi and G. J. W. Euverink, "Polyaniline functionalized electrochemically reduced graphene oxide chemiresistive sensor to monitor the pH in real time during microbial fermentations," *Sensors and Actuators B: Chemical*, vol. 264, pp. 38-44, 2018.

[67] A. Manaf, M. Hafizah, and A. Riyadi, "Electrical conductivity of polyaniline (PANI) assisted by anionic surfactant through emulsion polymerization technique," in *Journal of Physics: Conference Series*, 2019, vol. 1153, no. 1: IOP Publishing, p. 012067.

[68] H. D. Nguyen *et al.*, "pH sensitivity of emeraldine salt polyaniline and poly (vinyl butyral) blend," *Advances in Natural Sciences: Nanoscience and Nanotechnology*, vol. 5, no. 4, p. 045001, 2014.

[69] M. Tyona, "A theoritical study on spin coating technique," *Advances in materials Research*, vol. 2, no. 4, p. 195, 2013.

[70] H. Chiarini-Garcia and R. C. Melo, *Light microscopy*. Springer, 2011.

[71] D.-H. Lee and N.-G. Cho, "Assessment of surface profile data acquired by a stylus profilometer," *Measurement science and technology*, vol. 23, no. 10, p. 105601, 2012.

[72] G. Amorese, "LCR/impedance measurement basics," *Hewlett-Packard Company*, vol. 1997, 1997.

[73] Z. Ma *et al.*, "Highly sensitive, printable nanostructured conductive polymer wireless sensor for food spoilage detection," *Nano letters*, vol. 18, no. 7, pp. 4570-4575, 2018.

[74] S. Padmapriya, S. Harinipriya, K. Jaidev, V. Sudha, D. Kumar, and S. Pal, "Storage and evolution of hydrogen in acidic medium by polyaniline," *International Journal of Energy Research*, vol. 42, no. 3, pp. 1196-1209, 2018, doi: https://doi.org/10.1002/er.3920.

[75] H. Yeager and A. Steck, "Cation and water diffusion in Nafion ion exchange membranes: influence of polymer structure," *Journal of the Electrochemical Society*, vol. 128, no. 9, p. 1880, 1981.

[76] S. Tan and D. Bélanger, "Characterization and Transport Properties of Nafion/Polyaniline Composite Membranes," *The Journal of Physical Chemistry B*, vol. 109, no. 49, pp. 23480-23490, 2005/12/01 2005, doi: 10.1021/jp054724e.

[77] J. L. Worlinsky, S. Halepas, M. Ghandehari, G. Khalil, and C. Brückner, "High pH sensing with water-soluble porpholactone derivatives and their incorporation into a Nafion® optode membrane," *Analyst*, vol. 140, no. 1, pp. 190-196, 2015.

[78] P. J. Kinlen, J. E. Heider, and D. E. Hubbard, "A solid-state pH sensor based on a Nafion-coated iridium oxide indicator electrode and a polymer-based silver chloride reference electrode," *Sensors and Actuators B: Chemical*, vol. 22, no. 1, pp. 13-25, 1994.

[79] P. Awasthi, R. Mukherjee, S. P. O. Kare, and S. Das, "Impedimetric blood pH sensor based on MoS 2–Nafion coated microelectrode," *RSC advances*, vol. 6, no. 104, pp. 102088-102095, 2016.
[80] M. J. Schoening, A. Poghossian, T. Yoshinobu, and H. Lueth, "Semiconductor-based field-effect structures for chemical sensing," in *Advanced Environmental and Chemical Sensing Technology*, 2001, vol. 4205: SPIE, pp. 188-198.
[81] M. J. Schöning, M. Thust, M. Müller-Veggian, P. Kordoš, and H. Lüth, "A novel silicon-based sensor array with capacitive EIS structures," *Sensors and Actuators B: Chemical*, vol. 47, no. 1-3, pp. 225-230, 1998.
[82] S. Petrovic, "Analytical Electrochemistry," in *Electrochemistry Crash Course for Engineers*, S. Petrovic Ed. Cham: Springer International Publishing, 2021, pp. 85-92.
[83] S. Bause *et al.*, "Development of an iridium-based pH sensor for bioanalytical applications," *Journal of Solid State Electrochemistry*, vol. 22, no. 1, pp. 51-60, 2018/01/01 2018, doi: 10.1007/s10008-017-3721-1.
[84] C. Nie, A. Frijns, M. Zevenbergen, and J. d. Toonder, "An integrated flex-microfluidic-Si chip device towards sweat sensing applications," *Sensors and Actuators B: Chemical*, vol. 227, pp. 427-437, 2016/05/01/ 2016, doi: https://doi.org/10.1016/j.snb.2015.12.083.
[85] L. Manjakkal, S. Dervin, and R. Dahiya, "Flexible potentiometric pH sensors for wearable systems," *RSC advances*, vol. 10, no. 15, pp. 8594-8617, 2020.
[86] F. G. Biñas and F. Sevilla, "Molecularly imprinted potentiometric sensor for surfactant based on electrosynthesized polyaniline," *Acta Manilana*, vol. 62, pp. 61-67, 2014.
[87] Z. Ping, H. Neugebauer, J. Theiner, and A. Neckel, "Protonation and electrochemical redox doping processes of polyaniline in aqueous solutions: Investigations using in situ FTIR-ATR spectroscopy and a new doping system," *Journal of the Chemical Society, Faraday Transactions*, vol. 93, no. 1, pp. 121-129, 1997.
[88] D. Seo and J. Kim, "Effect of the Molecular Size of Analytes on Polydiacetylene Chromism," *Advanced Functional Materials*, vol. 20, no. 9, pp. 1397-1403, 2010, doi: https://doi.org/10.1002/adfm.201000262.
[89] S. K. Al-Hayali, A. M. Salman, and A. H. Al-Janabi, "Effect of hygroscopic polymer-coatings on the performance of relative humidity sensor based on macro-bend single-mode fiber," *Optical Fiber Technology*, vol. 62, p. 102460, 2021.
[90] A. Chanakul, N. Traiphol, and R. Traiphol, "Controlling the reversible thermochromism of polydiacetylene/zinc oxide nanocomposites by varying alkyl chain length," *Journal of colloid and interface science*, vol. 389, no. 1, pp. 106-114, 2013.
[91] H. E. Cingil, G. Beliktay, and E. M. Tan, "A study on the conformation-dependent colorimetric response of polydiacetylene supramolecules to external triggers," *Materials Chemistry Frontiers*, vol. 7, no. 2, pp. 294-305, 2023.